

Understanding many-body physics in one dimension from the Lieb-Liniger model

Y.-Z. Jiang,^{1,2} Y.-Y. Chen,^{1,2} and X.-W. Guan^{1,2,*}

¹*State Key Laboratory of Magnetic Resonance and Atomic and Molecular Physics,
Wuhan Institute of Physics and Mathematics, Chinese Academy of Sciences, Wuhan 430071, China*

²*Center for Cold Atom Physics, Chinese Academy of Sciences, Wuhan 430071, China*
(Dated: December 3, 2024)

This article presents an elementary introduction on various aspects of the prototypical integrable model the Lieb-Liniger Bose gas ranging from the cooperative to the collective features of many-body phenomena [1]. In 1963 Lieb and Liniger first solved this quantum field theory many-body problem using the Bethe's hypothesis, i.e. a particular form of wave function introduced by Bethe in solving the one-dimensional Heisenberg model in 1931. Despite the Lieb-Liniger model is arguably the simplest exactly solvable model, it exhibits rich quantum many-body physics in terms of the aspects of mathematical integrability and physical universality. Moreover, the Yang-Yang grand canonical ensemble description for the model provides us with a deep understanding of quantum statistics, thermodynamics and quantum critical phenomena at the many-body physics level. Recently, such fundamental physics of this exactly solved model has been attracting growing interest in experiments. Since 2004, there have been more than 20 experimental papers that report novel observations of different physical aspects of the Lieb-Liniger model in the lab. So far the observed results to date are seen to be in excellent agreement with results obtained using the analysis of this simplest exactly solved model. Those experimental observations reveal the unique beauty of integrability.

CONTENTS

I. Introduction	1
II. Bethe Ansatz for the Lieb-Liniger Bose gas	3
II.1 Wave function	3
II.2 Bethe ansatz equations	4
III. Ground state energy, excitations and correlations	4
III.1 Ground state: from cooperative to collective	5
Weak coupling limit: semicircle law	5
Strong coupling limit: fermionization	6
Elementary excitations: collective motion	6
The super Tonks-Girardeau gas like phase	8
III.2 Luttinger parameter and correlation functions	9
IV. Yang-Yang thermodynamics and quantum criticality	10
IV.1 The Yang-Yang grand canonical ensemble	10
IV.2 The Yang-Yang equation and quantum statistics	11
IV.3 Luttinger liquid and quantum criticality	12
Equation of state	12
Quantum criticality	13
IV.4 The local pair correlations and Tan's Contact	14
V. Experimental development related to the Lieb-Liniger gas	14
VI. Outlook	17
References	17

I. INTRODUCTION

Mathematical principles play significant roles in understanding quantum physics. The concept exact integrability originally came from the early study of the classical dynamical systems which were described by some differential equations. Usually, the solutions of those differential equations are tantamount to the determination of enough integration constants, i.e. the integrals of motions. In this sense, classical integrability is synonymous

with exact solution. However, conceptual understanding of quantum integrability should trace back to Hans Bethe's seminal work to obtain the energy eigenstates of the one-dimensional Heisenberg spin chain with the nearest interaction in 1931 [2]. He proposed a special form of the wavefunction - superposition of all possible permutations of plane waves in a ring of size L , namely

$$\chi = \sum_{\mathcal{P}} A(\mathcal{P}) e^{i(k_{\mathcal{P}_1} x_1 + \dots + k_{\mathcal{P}_N} x_N)}$$

where N is the number of down spins and $\mathcal{P}_1, \dots, \mathcal{P}_N$ stand for a permutation \mathcal{P} of $1, 2, \dots, N$. The $N!$ plane waves are N -fold products of individual exponential phase factors $e^{ik_i x_j}$. Here the N distinct wave numbers k_i , are permuted among the N distinct coordinates x_j . Each of the $N!$ plane waves have an amplitude coefficient which can be in turn determined by solving the eigenvalue problem of the Heisenberg Hamiltonian.

The Bethe's ansatz appeared to be escaped from the physicists' attention that time. It was only 30 years later that in 1963 Lieb and Liniger [3] first solved the one-dimensional (1D) many-body problem of delta-function interacting bosons by the Bethe's hypothesis. The exact solution for the delta-function interacting Bose gas was given in term of the wave numbers k_i with $i = 1, \dots, N$ satisfying a set of Bethe ansatz equations - called the Lieb-Liniger equations. The spectrum was given by summing up all k_i^2 . In fact, the Bethe ansatz equations describe the roles of individual particles played in many-body corrections. The significance of quantum integrability is such that the roles of individual particles enable one to precisely access full aspects of many-body physics for a particular universality class of many-body systems, for example, spin chains, interacting quantum gases, strongly correlated electronic systems, Kondo impurity problems,

Gaudin magnets etc.

Once concerning ensemble statistics, we have to properly distinguish physical origin of *distinguishable* and *indistinguishable* particles. At the room temperatures, the molecules in the air can be treated as a billiard balls that occasionally collide with each other. The size of those molecules is much smaller than the mean distance between them. The particles are *distinguishable*. However, according to de Broglie matter wave theory, the thermal wave length of a moving particles are given by simple formula $\lambda_{dB} = \sqrt{2\pi\hbar^2/(mk_B T)}$, here m is the mass of the particle, \hbar is the Plank constant, k_B is the Boltzmann constant and T is the temperature. The temperature goes to very low, the thermal wave length increase and the wave packets start overlap. Thus the particles are *indistinguishable* below the degenerate temperature. The quantum statistics play an essential role under such a degenerate temperature. Below the degenerate temperature, there are thus fundamental differences between the properties of fermions (with spins of $1/2, 3/2, \dots$) and bosons (with spins of $0, 1, 2, \dots$). All fermions must obey the Pauli exclusion principle, which means that they cannot occupy the same quantum state. However, as bosons are not subject to the same restrictions they can collapse under suitable conditions into the same quantum ground state, known as a Bose-Einstein condensate. The Lieb-Liniger model provides an ideal ensemble to understand the physics resulted in from the *distinguishable* and *indistinguishable* nature of classical and quantum particles.

Towards to a deeper understanding of the physics of the Lieb-Liniger gas, a significant next step was made by C N Yang and C P Yang on the thermodynamics of this many-body problem in 1969 [4]. They are for the first time to present a grand canonical description of the model in equilibrium. In fact, there are many microscopic states for an equilibrium state of the system at finite temperatures. The minimization of Gibbs free energy gives rise to the so-called Yang-Yang equation that determines the true physical state in an analytical way. In the grand canonical ensemble, the total number of particles can be changed associated with chemical potential μ . The temperature associate the entropy S , counting thermal disorder. This canonical Yang-Yang approach marks a significant step to the exact solutions of finite temperature many-body physics. It shows the subtlety of vacuum fluctuation, interaction effect, excitation modes, criticality, quantum statistics, thermalization, dynamics, correlations and Luttinger liquid.

The name Bethe's hypothesis was coined by Yang and Yang in the study of the Heisenberg spin chain. The Bethe ansatz is now well accepted as a synonym of quantum integrability. From solving eigenvalue problem of spin-1/2 delta-function interacting Fermi gas, C N Yang [5] found that the many-body scattering matrix can be reduced to a product of many two-body scattering ma-

trices, i.e. a necessary conditions for solvability of the 1D man-body systems. The two-body scattering matrix satisfies a certain intertwined relation, called Yang-Baxter equation. This seminal work has inspired great deal of developments in physics and mathematics. The Yang-Baxter relation was independently showed by R Baxter as the conditions for commuting transfer matrices in two-dimensional statistical mechanics [7]. For such exactly solved models, the energy eigenspectrum of the model Hamiltonian can be obtained exactly in terms of the Bethe ansatz equations, from which physical properties can be derived via mathematical analysis. The Lieb-Liniger Bose gas [3] and Yang-Gaudin model [5, 6] are both notable Bethe ansatz integrable models.

Yang-Baxter solvable models have flourished into majority in physics since last 70's. Later it turned out that the Yang-Baxter integrability play important roles in physical and mathematical study [8–15]. The Bethe ansatz approach has also found success in the realm of condensed matter physics, such as Kondo impurity problems, BCS pairing models, strongly correlated electron systems and spin ladders, cold atoms, quantum optics, quantum statistical mechanics, etc. The Yang-Baxter equation has led significant developments in mathematics such as in 2D conformal field theory, quantum groups, knot theory, and 2D statistical problems, lattice loop models, random walks, etc. Recent research shows that there exists a remarkable connection between conformal field theory and Yang-Baxter integrability of 2D lattice models. Remarkably, conformal field theory has led to the theory of vertex operator algebras, modular tensor categories and algebraic topology in connection to new states of matter with topological order, such as fractional quantum Hall effect, topological insulators etc. In this elementary introduction to the exactly solvable Lieb-Liniger model, we will discuss the rigorousness of mathematical integrability and the novelty of quantum many-body effects that comprise the beautiful cold world of many-body systems in the lab. The content of this article involves understanding the fundamental many-body physics through the model of Lieb-Liniger Bose gas.

The paper is organized as follows. In Section 2, we present a rigorous derivation of the Bethe ansatz for the Lieb-Liniger Bose gas. In this section we show how a field theory problem reduces to a quantum mechanic many-body systems following the Lieb-Liniger's derivation. In section 3, the ground state properties are discussed. Those include ground state energy, excitations, cooperative and collective features and Luttinger parameter etc. In Section 4, we introduce Yang-Yang grand canonical approach to the finite temperature physics of the Lieb-Liniger gas. In this section, we demonstrate how the Yang-Yang equation encode the subtle Bose-Einstein statistics, Fermi-Dirac statistics and Boltzmann statistics. In particular, we give an insightful understanding of quantum criticality. In section 5, we briefly review some

of recent experimental measurements related to the Lieb-Liniger Bose gas from which one can conceive the beauty of the integrability.

II. BETHE ANSATZ FOR THE LIEB-LINIGER BOSE GAS

II.1 Wave function

We start with introduction of canonical quantum Bose fields $\hat{\psi}(x)$ satisfying the following commutation relations

$$\begin{aligned} [\hat{\psi}(x), \hat{\psi}^\dagger(y)] &= \delta(x - y), \\ [\hat{\psi}(x), \hat{\psi}(y)] &= [\hat{\psi}^\dagger(x), \hat{\psi}^\dagger(y)] = 0. \end{aligned}$$

The Hamiltonian of the 1D single component bosonic quantum gas of N particles in a 1D box with length L is given by [3]

$$\hat{H} = \frac{\hbar^2}{2m} \int_0^L dx \partial_x \hat{\psi}^\dagger \partial_x \hat{\psi} + \frac{g_{1D}}{2} \int_0^L dx \hat{\psi}^\dagger \hat{\psi}^\dagger \hat{\psi} \hat{\psi}, \quad (1)$$

where m is the mass of the bosons, g_{1D} is the coupling constant which is determined by the 1D scattering length $g_{1D} = -2\hbar^2/ma_{1D}$. The scattering length is given by $a_{1D} = (-a_\perp^2/2a_s) [1 - C(a_s/a_\perp)]$ [28]. Here the numerical constant $C \approx 1.4603$. The model (1) presents the second-quantized form of the Lieb-Liniger Bose gas with contact interaction [3].

In order to process Lieb and Liniger's solution, we first define the vacuum state in the Fock space as $\hat{\psi}(x)|0\rangle = 0$, $x \in \mathbb{R}$ with $\langle 0 | 0 \rangle = 1$. The equation of motion for the field $\hat{\psi}(x)$ is given by the Heisenberg equation $i\partial_t \hat{\psi}(x) = [\hat{H}, \hat{\psi}(x)]$. It follows that the corresponding equation of the motion for this model reads

$$i\partial_t \hat{\psi}(x) = -\partial_x^2 \hat{\psi}(x) + 2c\hat{\psi}^\dagger(x)\hat{\psi}(x)\hat{\psi}(x). \quad (2)$$

Considering $\hat{\psi}(x)$ as a classical field, this equation of motion reduces to a non-linear Schrödinger equation of the classical field theory. Moreover, it is easy to show that the particle number operator \hat{N} and the momentum operator \hat{P}

$$\hat{N} = \int_0^L \hat{\psi}^\dagger \hat{\psi} dx, \quad \hat{P} = -\frac{i}{2} \int_0^L \left\{ [\partial_x, \hat{\psi}^\dagger(x)] \hat{\psi}(x) \right\} dx. \quad (3)$$

are commutative with the Hamiltonian (1), i.e. $[\hat{H}, \hat{N}] = 0$ and $[\hat{H}, \hat{P}] = 0$. They are among the conserved quantities of this model.

The eigenfunction of the N -particle state $|\Psi\rangle$ for the operators \hat{H} , \hat{N} and \hat{P} is given by

$$|\Psi\rangle = \frac{1}{\sqrt{N!}} \int_0^L d^N \mathbf{x} \Psi(\mathbf{x}) |\mathbf{x}\rangle, \quad (4)$$

where $\mathbf{x} = \{x_1, x_2, \dots, x_N\}$ and $|\mathbf{x}\rangle = \hat{\psi}^\dagger(x_1)\hat{\psi}^\dagger(x_2)\dots\hat{\psi}^\dagger(x_N)|0\rangle$. Here x_j is the coordinate position of the j -th particle. For the bosons, the first quantized wave function Ψ is symmetric with respect to any exchange of two particles in space \mathbf{x} , namely

$$\Psi(\dots, x_\xi, \dots, x_\eta, \dots) = \Psi(\dots, x_\eta, \dots, x_\xi, \dots). \quad (5)$$

In the following discussions, we set $\hbar = 2m = 1$ and $c = mg_{1D}/\hbar^2$. After some algebra, one can find that the eigenvalue problem of the Schrödinger equation $\hat{H}|\Psi\rangle = E|\Psi\rangle$ in N -particle sector reduces to the quantum mechanic man-body problem which is described by the Schrödinger equation $H\Psi(\mathbf{x}) = E\Psi(\mathbf{x})$ with the first quantized form of the Hamiltonian

$$H = -\sum_{i=1}^N \frac{\partial^2}{\partial x_i^2} + 2c \sum_{i < j} \delta(x_i - x_j). \quad (6)$$

This many-body Hamiltonian describes N bosons with δ -function interaction in one dimension—called the Lieb-Liniger model. This is a physical realistic model in quantum degenerate gases with s -wave scattering potential. In the dilute quantum gases, when the average distance between particles is much larger than the scattering length, the s -wave scattering between two particles at x_ξ and x_η have the following short distance behaviour [16]

$$\Psi'(0^+) - \Psi'(0^-) = -\frac{1}{a_{1D}} [\Psi(0^+) + \Psi(0^-)], \quad (7)$$

where $\Psi(x)$ in Eq. (7) is the relative wave function of the two particles and x is the relative distance between the two particles, i.e. $x = x_\eta - x_\xi$. In the above equation, the prime denotes the derivative with respect to x .

In the model (6), the interaction only occurs when two particles contact with each other. Following the Bethe ansatz [2] we can divide the wave function into $N!$ domains according to the positions of the particles $\Theta(\mathcal{Q}) : x_{\mathcal{Q}_1} < x_{\mathcal{Q}_2} < \dots < x_{\mathcal{Q}_N}$, where \mathcal{Q} is the permutation of number set $\{1, 2, \dots, N\}$. The wave function can be written as $\Psi(\mathbf{x}) = \sum_{\mathcal{Q}} \Theta(\mathcal{Q}) \psi_{\mathcal{Q}}(\mathbf{x})$. Considering the symmetry of bosonic statistics, all the ψ in different domain \mathcal{Q} should be the same, i.e., $\psi_{\mathcal{Q}} = \psi_1$, where we use $\mathbf{1}$ denote the unitary element of the permutation group, $\mathbf{1} = \{1, 2, \dots, N\}$. Lieb and Liniger wrote the wave function for the model (6) as the superposition of $N!$ plane waves [3]

$$\psi_1 = \sum_{\mathcal{P}} A(\mathcal{P}) e^{i(k_{\mathcal{P}_1} x_1 + \dots + k_{\mathcal{P}_N} x_N)}, \quad (8)$$

where k s are the pseudo-momenta carried by the particles under a periodic boundary conditions.

Indeed, after solving the Schrödinger equation $H\Psi(\mathbf{x}) = E\Psi(\mathbf{x})$, we can get the same s -wave scattering boundary condition (7) that provides the two-body scattering relation among the coefficients $A(\mathcal{P})$

$$A(\mathcal{P}') = \frac{k_{\mathcal{P}_j} - k_{\mathcal{P}_{j+1}} + ic}{k_{\mathcal{P}_j} - k_{\mathcal{P}_{j+1}} - ic} A(\mathcal{P}), \quad (9)$$

where \mathcal{P}' is a permutation obtained by exchanging \mathcal{P}_j and \mathcal{P}_{j+1} , i.e., $\mathcal{P}' = \{\mathcal{P}_1, \dots, \mathcal{P}_{j-1}, \mathcal{P}_{j+1}, \mathcal{P}_j, \mathcal{P}_{j+2}, \dots, \mathcal{P}_N\}$. The scattering process in Eq. (9) implies that any two-body scattering with momenta k_a and k_b leads to an anti-symmetric phase shift $A(\mathcal{P}') = e^{-i\theta(k_{\mathcal{P}_j} - k_{\mathcal{P}_{j+1}})} A(\mathcal{P})$,

$$\theta(k_a - k_b) = 2\arctan\left(\frac{k_a - k_b}{c}\right). \quad (10)$$

When $c \neq 0$, all the quasi-momenta are different. If there are two equal pseudo momenta $k_a = k_b$, we can prove that the wave function $\psi_{\mathbb{1}} = 0$.

In general, the Eq. (9) gives the two-body scattering matrix \hat{S} , $A(\mathcal{P}') = \hat{S}A(\mathcal{P})$ for a quantum many-body system. C. N. Yang [5] proved that, if the two-body scattering matrix \hat{S} satisfies the following equation

$$\hat{S}_{12}(\lambda - \mu)\hat{S}_{13}(\lambda)\hat{S}_{23}(\mu) = \hat{S}_{23}(\mu)\hat{S}_{13}(\lambda)\hat{S}_{12}(\lambda - \mu), \quad (11)$$

then the system is integrable. This relation was independently found by R. Baxter [7] in studying two-dimensional statistical models. In nowadays the equation (11) is called *Yang-Baxter equation*. The Yang-Baxter equation guarantees that the multi-body scattering process can be factorized as the product of many two-body scattering processes. This factorization reveals the nature of the integrability, i.e. no diffraction in outgoing wave. For the Lieb-Liniger model (6), \hat{S} matrix is a scalar function so that the scattering matrix satisfies the Yang-Baxter equation trivially. In the scattering process from $\mathbb{1}$ to \mathcal{P} , the multi-body scattering matrix is defined by $A(\mathcal{P}) = \hat{S}(\mathcal{P}\mathbf{k})A(\mathbb{1})$. By using Eq.(9), the multi-body scattering matrix of this model is given by

$$\hat{S}(\mathcal{P}\mathbf{k}) = \prod_{\mathcal{P}_j < \mathcal{P}_l} \frac{k_{\mathcal{P}_j} - k_{\mathcal{P}_l} - ic}{k_{\mathcal{P}_j} - k_{\mathcal{P}_l} + ic}. \quad (12)$$

With the help of the Eq. (12), the eigen wavefunction of the system is given by

$$\Psi(\mathbf{x}) = \sum_{\mathcal{Q}, \mathcal{P}} \Theta(\mathcal{Q}) \left(\prod_{\mathcal{P}_j < \mathcal{P}_l} \frac{k_{\mathcal{P}_j} - k_{\mathcal{P}_l} - ic}{k_{\mathcal{P}_j} - k_{\mathcal{P}_l} + ic} \right) e^{i\mathcal{Q}\mathbf{x} \cdot \mathcal{P}\mathbf{k}}. \quad (13)$$

II.2 Bethe ansatz equations

Submitting the periodic boundary conditions $\Psi(\dots, x_{\xi} = 0, \dots) = e^{i\alpha}\Psi(\dots, x_{\xi} = L, \dots)$ into the wave function (13), we can find that the pseudo momenta k_l satisfies the following Bethe ansatz equations (BAE)

$$e^{ik_i L} = -e^{-i\alpha} \prod_{j=1}^N \frac{k_i - k_j + ic}{k_i - k_j - ic}, \quad i = 1, 2, \dots, N, \quad (14)$$

which are called the *Lieb-Liniger equations*. When $\alpha = \pi$, the wave function is anti-periodic; while when $\alpha = 0$, it

is periodic. In the following discussion, we only consider the periodic boundary conditions.

Since partial number \hat{N} and momentum \hat{P} are conserved quantities of the Lieb-Liniger model, the Hamiltonian together with \hat{N} and \hat{P} can be simultaneously diagonalized. For the eigenstate (13), the corresponding particle number $\langle \hat{N} \rangle = N$. For a given set of quasi-momenta $\{k_j\}$, the total momentum and the energy of the system are obtained

$$P = \langle \hat{P} \rangle = \sum_j^N k_j, \quad E = \langle \hat{H} \rangle = \sum_j^N k_j^2. \quad (15)$$

The solutions to the BAE (14) provide complete spectra of the Lieb-Liniger model. The physical solutions to the Bethe ansatz equations require that all the pseudo momenta are distinct to each other. The BAE (14) can be written in the form of phase shift function $\theta(k)$:

$$2\pi \frac{I_i}{L} = k_i + \frac{1}{L} \sum_{j=1}^N \theta\left(\frac{k_i - k_j}{c}\right), \quad (16)$$

where $\{I_i\}$ are the quantum numbers of pseudo momenta. If N is odd, these quantum numbers are integers, whereas they are half odd integers when N is even. For a given set of quantum numbers $\{I_i\}$, there is a unique set of real values $\{k_i\}$ for $c > 0$. These quantum numbers are independent of coupling constant c . The total momentum can be expressed as

$$P = \frac{2\pi}{L} \sum_{i=1}^N I_i = 2\ell\pi/L, \quad \ell = 0, \pm 1, \pm 2, \dots \quad (17)$$

For the ground state $P = 0$, where all quasi-momenta $\{k_i\}$ locate in an interval $(-Q, Q)$. Here Q is the cut-off. For the ground state, the quantum numbers are given by

$$I_j = -\frac{N-1}{2} + j - 1, \quad j = 1, \dots, N. \quad (18)$$

III. GROUND STATE ENERGY, EXCITATIONS AND CORRELATIONS

In the thermodynamic limit, i.e. $N, L \rightarrow \infty$ and the particle density $n = N/L$ is a constant, the BAE (16) can be written in the integral form

$$\rho(k) = \frac{1}{2\pi} - \int_{-Q}^Q a(k-q)\rho(q)dq, \quad |k| < Q. \quad (19)$$

Where $\rho(k)$ is the density distribution function of the quasi-momenta defined by the particle numbers in a small interval of $(k, k + \Delta k)$, i.e.

$$\rho(k) = \lim_{\Delta k \rightarrow 0} \frac{1}{L\Delta k}.$$

Here the cut-off Q is the “Fermi point” of the pseudo momenta. It is determined by the particle density $n = \int_{-Q}^Q \rho(k) dk$. Energy per length can also be written as

$$\frac{E}{L} = \int_{-Q}^Q \rho(k) k^2 dk. \quad (20)$$

For the ground state the energy depends on the dimensionless scale $\gamma = Lc/N$. Let's make a scaling transformation

$$k = Qx, \quad c = Q\lambda, \quad \rho(Qx) = g(x), \quad (21)$$

we find the ground state energy per particle,

$$\frac{E}{N} = \frac{\hbar^2 n^2}{2m} e_0(\gamma) \quad (22)$$

with $e_0(\gamma) = \frac{\gamma^3}{\lambda^3} \int_{-1}^1 x^2 g_0(x) dx$. Where the distribution function $g_0(x)$ is determined by

$$g_0(x) = \frac{1}{2\pi} + \frac{\lambda}{\pi} \int_{-1}^1 \frac{g_0(y)}{\lambda^2 + (x-y)^2} dy \quad (23)$$

with the cut-off condition $\gamma \int_{-1}^1 g_0(x) dx = \lambda$. The equation (23) is the standard inhomogeneous Fredholm equation, which is well understood in mathematics. The Fredholm equation can be numerically solved. We will further study the ground state energy later.

III.1 Ground state: from cooperative to collective

For the ground state, the competition of kinetic energy and interaction energy is represented by the dimensionless coupling strength γ . When $\gamma = 0$, the system is free bosons, all the particles condensed at the zero momentum state while if there is a small coupling constant, all the k s are distinct. At the limit $\gamma = \infty$, the strong repulsion makes the quasi-momentum distribution the same as the one of the free fermions.

Weak coupling limit: semicircle law

It is very insightful to examine the physics of the model in weak coupling limit. In this case the Bethe ansatz roots comprise the semi-circle law. Gaudin firstly noticed such a kind of distribution [17]. Later it was found by several groups [18, 19]. The Fredholm equation (23) is known as the Love equation for the problem of the circular disk condenser. By using Hutson's method, Gaudin found the density distribution function and energy density

$$g_0(t) \approx \frac{Q}{2\pi c} (1 - t^2)^{\frac{1}{2}}$$

$$+ \frac{1}{4\pi^2} (1 - t^2)^{-\frac{1}{2}} \left(t \ln \frac{1-t}{1+t} + \ln \frac{16\pi e Q}{c} \right),$$

$$e = n^3 \left(\gamma - \frac{4}{3\pi} \gamma^{3/2} \right), \quad (24)$$

This result coincides with the perturbative calculation by using Bogoliubov method.

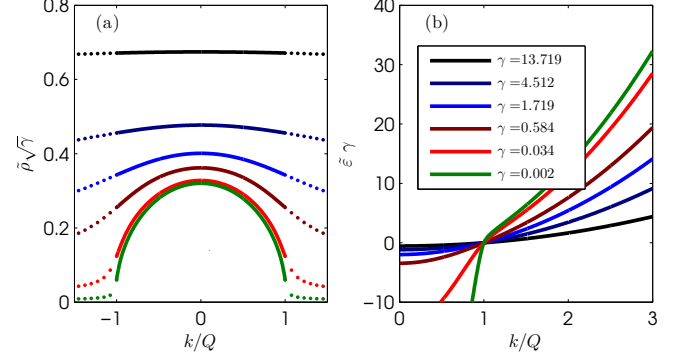


FIG. 1. (Color online) Densities and dressed energies of pseudo momenta for the ground state. (a), The solid lines are the dimensionless densities of the pseudo momenta, $\tilde{\rho}(k) = \rho(k)/c$ obtained from the eq (23). Whereas the dotted lines are the corresponding dimensionless hole densities, $\tilde{\rho}_h(k) = \rho_h(k)/c$. When the coupling strength is small, the distribution function $\tilde{\rho}$ meets a semi-circle law (27). For the strong coupling limit, i.e. $\gamma \gg 1$, the distribution function gradually becomes flatter and flatter, towards to $\rho(k) \approx 1/2\pi$. (b), Dimensionless dressed energy is defined by $\tilde{\varepsilon}(k) = \varepsilon(k)/c^3$ which is obtained from the dressed energy equation (64).

This problem can also be solved from the original BAE (14). In the weak coupling limit, i.e. $Lc \ll 1$, the quasi-momenta k_j are proportional to the square root of c and $c/(k_j - k_l)$ is a small value. Up to the second order of c , the BAE (14) is expanded as [19]

$$q_j = \sum_{l \neq j}^N \frac{1}{q_j - q_l}, \quad (25)$$

where $q_j = k_j \sqrt{L/2c}$. If we define a function $H_N(q) = \prod_{i=1}^N (q - q_i)$, we can find that $F(q_j) = 0$ for the polynomial $F(q) \equiv H_N''(q) - 2qH_N'(q)$. Both $F(q)$ and $H_N(q)$ are the polynomial of degree N and $F(q_j) = H_N(q_j) = 0$, $F(q)$ and $H_N(q)$ are proportional to each other. At the large order of q , $H(q) = q^N + \dots$ and $F(q) = -2Nq^N + \dots$, so that we have $F(q) = 2NH_N(q)$. It follows that

$$H_N''(q) - 2qH_N'(q) + 2NH_N(q) = 0. \quad (26)$$

The solution of this differential equation is a Hermite polynomial and q_j is the root of the corresponding polynomial of degree N , i.e. $H_N(q) = 0$. We set the order of q_j as $q_j < q_{j+1}$, then we have $(2N + 1 - q_j^2)^{1/2} >$

$\pi/(q_{j+1}-q_j) > (2N+1-q_{j+1}^2)^{1/2}$. The distribution function, $\rho(k) = \lim_{L,N \rightarrow \infty} \frac{1}{L(k_{j+1}-k_j)}$ is thus determined by [20]

$$\rho(k) \approx \frac{1}{\pi} \sqrt{\frac{n}{c}} \left(1 - \frac{k^2}{Q^2}\right)^{1/2} + O\left(\frac{1}{Lnc}\right), \quad (27)$$

where the cut-off $Q = 2\sqrt{nc}$ is obtained by $\int_{-Q}^Q \rho(k) dk = n$. We can see that the quasimomentum distribution function satisfy the the semi-circle law where the cut-off is the radius of this circle, see Fig. 1 (a). The leading order of energy (24) was also found based on the pseudo momentum distribution (27).

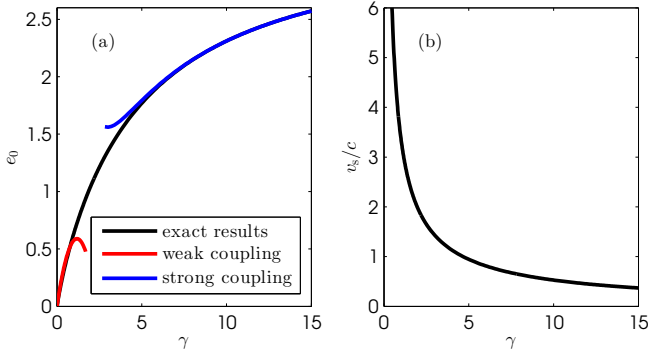


FIG. 2. (Color online) The ground state energy and sound velocity for different coupling strength γ . (a), The ground energy density is a monotonic increasing function of γ when the linear density is fixed. The black line is the exact numerical result from Eq. (23). The red line is the the weakly coupling expansion result Eq. (24). Whereas the blue line is the result obtained by the strongly coupling expansion Eq. (31). (b), The sound velocity is a monotonic decreasing function of γ . In the weakly coupling limit, the ratio turns to infinite, while at the strong coupling limit, $v_s/c \rightarrow 2\pi/\gamma$, see Eq. (45).

Strong coupling limit: fermionization

In the strong repulsion limit, the gas is known as the Tonks-Girardeau (TG) gas. In realistic experiment with cold atoms, it is practicable to observe the quantum degenerate gas with the strong coupling regime [22, 23]. In the regime $\gamma \rightarrow \infty$, the Bose-Fermi mapping method [16] can map out the ground state properties of the Bose gas through the wave function of the non-interacting fermions. For finitely strong interaction, $\gamma \gg 1$, we can obtain the ground state pseudo momenta from the Bethe ansatz equations (14) [26, 33]

$$k_j = 2\pi \frac{I_j}{L} \left(1 - \frac{2}{\gamma} + \frac{4}{\gamma^2} - \frac{8}{\gamma^3}\right) + \frac{4\pi^3}{3c^3 L^4} \left[\left(N + \frac{1}{2} - j\right)^4 - \left(\frac{1}{2} - j\right)^4 \right] + O\left(\frac{1}{c^5}\right), \quad (28)$$

where I_j take the ground state quantum numbers $I_j = -\frac{N-1}{2} + j - 1$, $j = 1, \dots, N$. With the help of the Eq. (28), the ground state energy of the the strong repulsive gas is given by

$$\frac{E}{L} \approx \frac{\pi^2}{3} n^3 \left[1 - \frac{4}{\gamma} + \frac{12}{\gamma^2} + \frac{32}{\gamma^3} \left(\frac{\pi^2}{15} - 1 \right) \right], \quad (29)$$

This asymptotic result fits well the numerical result obtained by solving the the integral BAE (19), see Fig. 2 (a). The ground state energy (29) can also be obtained from the integral BAE (19) by strong coupling expansion method [26, 69]. We see that for $\gamma \rightarrow \infty$ the leading order of the ground state energy reduces to the one of the free fermions $e_f = \pi^2 n^3 / 3$. One can also calculate other important properties such as compressibility, sound velocity, Luttinger parameter once we know the dimensionless function $E(\gamma)$.

Very recently, Ristivojevic obtained high precision ground state distribution function for the strong coupling regime [69]

$$\rho(k) = \frac{1}{2\pi} + \frac{1}{\pi^2 \lambda} + \frac{2}{\pi^3 \lambda^2} + \frac{12 - \pi^2}{3\pi^4 \lambda^3} + \frac{8 - 2\pi^2}{\pi^5 \lambda^4} - \frac{k^2}{Q^2} \left(\frac{1}{\pi^2 \lambda^3} + \frac{1}{\pi^3 \lambda^4} \right) + O(\lambda^{-5}). \quad (30)$$

The ground state energy per unit length and particle density are given by

$$\frac{E}{L} = \frac{\lambda^3}{3\pi c^3} \left(1 + \frac{2}{\pi \lambda} + \frac{4}{\pi^2 \lambda^2} + \frac{120 - 28\pi^2}{15\pi^3 \lambda^3} + \frac{80 - 26\pi^2}{5\pi^4 \lambda^4} \right), \quad (31)$$

$$n = \frac{\lambda}{c\pi} \left(1 + \frac{2}{\pi \lambda} + \frac{4}{\pi^2 \lambda^2} + \frac{24 - 4\pi^2}{3\pi^3 \lambda^3} + \frac{48 - 14\pi^2}{3\pi^4 \lambda^4} \right), \quad (32)$$

where $\lambda = (\gamma + 2)/\pi - 4\pi/(3\gamma^2) + 16\pi/(3\gamma^3)$. The result $e_0 = E/(Ln^3)$ is plotted in Fig. 2.

Elementary excitations: collective motion

As being discussed in previous section, the eigenstates of the model are described by the quantum numbers $\{I_j\}$. We define I_j as a function of the pseudomomenta, i.e. $I(k_j) = I_j$, thus we have

$$\frac{I(k)}{L} = \frac{k}{2\pi} + \frac{1}{L} \sum_{j=1}^N \frac{\theta(k - k_j)}{2\pi}. \quad (33)$$

Usually we define the occupied Bethe ansatz roots as particles while the unoccupied roots as holes. For a hole quasimomentum k_h , the quantum number $I_h = I(k_h) \in \mathbb{Z} + (N+1)/2$. We demonstrate the quantum numbers I_j for the ground state and excited states in Fig. 3 (a)-(d). For the ground state, there is no hole below the quasi-Fermi-momentum, i.e., $|k| < Q$, whereas the quantum

numbers I_s for the holes site outside the interval $[I_1, I_N]$, see the Fig. 3 (a).

In the thermodynamic limit, the pseudo momentum distribution function $\rho_0(k)$ for the ground state is determined by the Eq. (19) with the cut-off as Q . The ground state energy and the particle density can be regarded as the function of the cut-off Q :, i.e. $e(Q)$ and $n(Q)$. The changes over the configuration of quantum numbers for ground state give rise to excited states. Fig. 3 (d) shows such an excitation where the particle with a quasimomentum k_h below the pseudo Fermi point is excited outside the Fermi point with a new quasimomentum k_e .

For a single particle excitation, we decompose the pseudo momentum density into two parts, $\rho_t(k) = \bar{\rho}(k) + \frac{1}{L}\delta(k - k_e)$, where the delta function term attributes to the excited particle and $\bar{\rho}(k)$ stands for the density below the cut-off pseudo momenta, i.e. $|k| < Q$. In the thermodynamic limit, $\bar{\rho}(k)$ satisfy the following integral equation

$$\bar{\rho}(k) = \frac{1}{2\pi} + \int_{-Q}^Q a(k - k')\bar{\rho}(k')dk' + \frac{1}{L}a(k - k_e). \quad (34)$$

Here we chose a state satisfies Eq. (19) with cut-off Q as a reference state, i.e.

$$\rho_0(k) = \frac{1}{2\pi} + \int_{-Q}^Q a(k - k')\rho_0(k')dk' + \frac{1}{L}a(k - k_e). \quad (35)$$

The addition of the excited particle leads to a collective rearrangement of the distribution of the pseudo momenta of the $N - 1$ particles. We denote the difference of the pseudo momentum distribution functions between the excited and the reference state as $\Delta\rho(k) = \bar{\rho}(k) - \rho_0(k)$, here $\rho_0(k)$ is the pseudo momentum distribution of the reference state within $|k| < Q$. By comparing the integral BAE (34) and (19), we can find that $\Delta\rho$ satisfies the following equation,

$$\Delta\rho(k) = \frac{1}{L}a(k - k_e) + \int_{-Q}^Q a(k - k')\Delta\rho(k')dk'. \quad (36)$$

The addition of the particle also leads to a shift of the cut-off over the pseudo-Fermi point of the ground state of N -particle, i.e. $\Delta Q = Q - Q_G$. Here, Q_G is the cut-off of for the ground state with the particle number $N = Ln_G(Q_G)$ and Q is the one for the excited state with $N = Ln_G(Q) + L \int_{-Q}^Q dk \Delta\rho(k) + 1$. At the thermodynamic limit, ΔQ is a small value. By comparing the formulas of particle numbers between the ground state and the excited state, $\Delta Q n'_G(Q_G) = -[\int_{-Q}^Q \Delta\rho(k)dk + 1/L]$. The prime denotes the derivative with respect to the the cut-off Q . The corresponding excited energy

$$\Delta E(k_e) = L \int_{-Q}^Q \Delta\rho(k)k^2 dk + k_e^2 + Le'(Q)\Delta Q$$

$$= L \int_{-Q}^Q \Delta\rho(k)(k^2 - \mu)dk + (k_e^2 - \mu), \quad (37)$$

where μ is the chemical potential, $\mu = dE/dN = e'_G(Q_G)/n'_G(Q_G)$. Later we will further prove that the dressed energy can be expressed as as

$$\varepsilon(k) = k^2 - \mu + \int_{-Q}^Q a(k - k')\varepsilon(k')dk'. \quad (38)$$

For convenience we introduce an useful relations between the dressed energy and density. Assuming that two functions $f(k)$ and $g(k)$ satisfy the following equations

$$\begin{aligned} f(k) &= f_0(k) + \int_{-Q}^Q a(k - k')f(k')dk', \quad |k| < Q, \\ g(k) &= g_0(k) + \int_{-Q}^Q a(k - k')g(k')dk', \quad |k| < Q, \end{aligned} \quad (39)$$

where $f_0(k)$ and $g_0(k)$ are the driving term of these integral equations. Then we have the useful relation

$$\int_{-Q}^Q f(k)g_0(k)dk = \int_{-Q}^Q g(k)f_0(k)dk. \quad (40)$$

By using the formula (40), form Eq. (38) and Eq. (19), we thus prove that the dressed energy is nothing but the excitation energy of a particle:

$$\begin{aligned} \varepsilon(k_e) &= k_e^2 - \mu + \int_{-Q}^Q a(k_e - k')\varepsilon(k')dk' \\ &= k_e^2 - \mu + L \int_{-Q}^Q (k_e^2 - \mu)\Delta\rho(k')dk' = \Delta E(k_e). \end{aligned} \quad (41)$$

On the other hand, the hole excitations impose an additional condition, namely the maximum momentum is $n\pi$. Similarly, one can prove that the excited energy reads

$$\Delta E(k_h) = -\varepsilon(k_h). \quad (42)$$

We plot the dressed energies for different coupling strength in Fig. 1 (b). In order to see clearly excitation spectra, we need to calculate the total momentum through the Eq. (17). For both the particle-hole excitation and the Type II hole excitation, the total particle numbers of particles do not change, Fig. 3 (d) and Fig. 4 (b). Therefore the total momenta of the excited states are given by

$$P = n\pi - 2\pi \int_0^{k_{e,h}} \rho_0(k)dk. \quad (43)$$

For the low-energy excitations, $k_e - Q$ is a very small value. Therefore the low-lying behavior can be described by a linear dispersion relation

$$\Delta E = \varepsilon'_G(Q)|k \pm Q| = v_s|P|, \quad v_s = \frac{\varepsilon'_G(Q)}{2\pi\rho_G(Q)}, \quad (44)$$

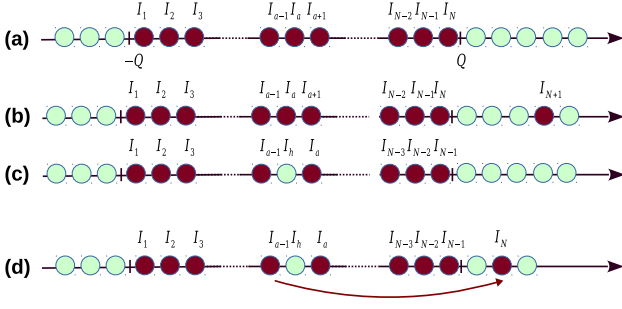


FIG. 3. (Color online) Schematic diagrams of the ground state and elementary excitations. (a) shows the quantum numbers for the ground state. The quantum numbers for the ground state are symmetric around the the origin. The largest quasi-momentum denotes the “Fermi points” $\pm Q$. (b) shows the configuration of adding a particle near right Fermi point with the quantum number I_{N+1} . So that the total number of particles is $N + 1$. (c) indicates a hole excitation. The hole at I_h is created so that the total number of particles is $N - 1$. In (b) and (c), the parities of their quantum numbers are changed from half-odd (or integers) to integer (or half-odds) due to the changes of particle numbers. (d) demonstrates a single particle-hole excitation. A particle at the position I_h is excited out of the pseudo Fermi sea. In this case, the total number of particles is still N , the parity of quantum numbers dose not change.

where v_s is the sound velocity of the system. In the above equation, \pm corresponds to the excitations at left/right Fermi point, respectively. Nevertheless, for $|k| > Q$, the relation (44) is the dispersion relation for particle-hole excitations. This linear spectra uniquely determine the universal Luttinger liquid behaviour at the low temperatures. The essential feature resulted from the dispersion relation (44) is such that the system exhibits the conformal invariant in low energy sector. We will further discuss this universal nature of the 1D many-body physics. For the strong coupling, we can get the sound velocity from the ground state energy through the relation $v_s = \sqrt{\frac{L}{mn} \frac{\partial^2 E}{\partial L^2}}$, namely,

$$v_s \approx 2\pi n \left[1 - \frac{4}{\gamma} + \frac{12}{\gamma^2} + \frac{16}{\gamma^3} \left(\frac{\pi^2}{3} - 2 \right) \right]. \quad (45)$$

In Fig. 2 (a) and (b), we present the analytical and numerical result for the dimensionless energy $\bar{e}(\gamma) = e/n^3$ and v_s/c , respectively.

The super Tonks-Girardeau gas like phase

In regard of the strong interacting bosons in 1D, the super Tonks-Girardeau gas is particularly interesting. It describes a gas-like phase of the attractive Bose gas which was first proposed in a system of attractive hard rods by

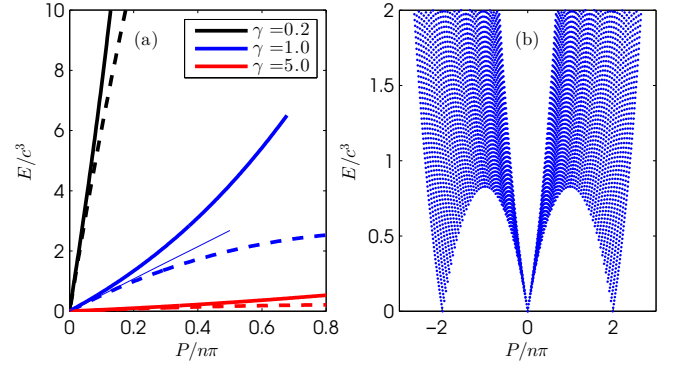


FIG. 4. (Color online) Dispersion relations in elementary excitations: adding one particle and adding one hole excitation. (a), The solid lines show the spectra for adding one particle to the ground state corresponding the configuration presented in the Fig. 3 (b). The dashed lines are the dispersion relations for the hole excitation, see the configuration given in Fig. 3 (c). For $\gamma = 1$, the thin blue line is calculated by using Eq. (44). We see that both the particle and hole excitations comprise the dispersion relations with the same velocity. (b) show the particle-hole excitation spectra, see Fig. 3 (d). The linear dispersion relation is seen for the long-wave leng limit, i.e. the momentum tends to zero.

Astrakharchik *et al.* [62]. Batchelor and his coworkers showed its existence of such a novel state in the Lieb-Liniger model with a strong attraction [63]. Due to the large kinetic energy inherited from the repulsive Tonks-Girardeau gas, the hard core behavior of the particles with Fermi-like pressure prevents the collapse of the super TG phase after the switch of interactions from repulsive to attractive interactions [64–67]. In fact, the energy can be continuous in the limits $c \rightarrow \pm\infty$. From the Bethe ansatz equations (14), near $c \rightarrow \pm\infty$, the compressibility is given by

$$\frac{1}{\kappa} = 2\pi^2 n - \frac{16\pi^2}{c} n^2 + \frac{80\pi^2}{c^2} n^3 + \left(\frac{64}{3}\pi^2 - 320 \right) \frac{n^4}{c^3}. \quad (46)$$

However, for the Lieb-Liniger gas with weak repulsive interaction ($0 < c \ll 1$), compressibility is given by

$$\frac{1}{\kappa} = 2c - \frac{1}{\pi\sqrt{n}} c^{3/2}. \quad (47)$$

In contrast, the energy for the gas-like phase (super Tonks-Girardeau gas) in weak attractive interaction limit ($-1 \ll c < 0$) is given by

$$E = \frac{2\pi^2}{3} n^2 - |c| n^2. \quad (48)$$

Thus the compressibility of the super Tonks-Giraread gas with weak attraction is given by

$$\frac{1}{\kappa} = 4\pi^2 n - 2|c|. \quad (49)$$

Such different forms of compressibility reveal an important insight on the root patterns of the quasi-momenta. We now show the subtlety of the Bethe ansatz roots for the super Tonks-Girardeau state in Fig.5.

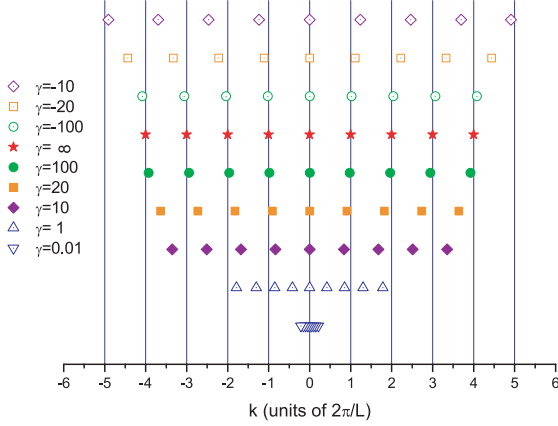


FIG. 5. (Color online) Quansimomenta for the ground state of the Lieb Liniger gas with the strongly repulsion and the super Tonks-Girardeau gas of the attractive Bose gas for a large value of γ . It is obvious that the super Tons-Girardeau gas has a larger kinetic energy than the free Fermion momentum.

III.2 Luttinger parameter and correlation functions

The 1D integrable system gives rise to the power law behaviour of long distance or long time asymptotics of correlation functions for the ground state. The effective Hamiltonian can be approximately described by the conformal Hamiltonian which can be written in terms of the generators of the underlying Virasoro algebra with the central charge $C = 1$. The low-lying excitations present the phonon dispersion $\Delta E(p) = v_s p$ in long-wave length limit. In this limit, all particles participate the excitations and form a collective motion of bosons which is called the Luttinger liquid [74]. The Lieb-Liniger field theory Hamiltonian can be rewritten as an effective Hamiltonian in long wave length limit, which essentially describes the low energy physics of the Lieb-Linger Bose gas

$$H = \int dx \left(\frac{\pi v_s K}{2} \Pi^2 + \frac{v_s}{2\pi K} (\partial_x \phi)^2 \right), \quad (50)$$

where the canonical momenta Π conjugate to the phase ϕ obeying the standard Bose commutation relations $[\phi(x), \Pi(y)] = i\delta(x - y)$. $\partial_x \phi$ is proportional to the density fluctuations. In this effective Hamiltonian, v_s/K fixes the energy for the change of density. In this approach, the density variation in space is viewed as a superposition of harmonic waves.

For example, the leading order of one-particle correlation $\langle \psi^\dagger(x)\psi(0) \rangle \sim 1/x^{1/2K}$ is uniquely determined by the Luttinger parameter K . The Luttinger parameter is defined by the ratio of sound velocity to stiffness, namely

$$K = \frac{v_s}{v_N} = \frac{\pi}{\sqrt{3e_0(\gamma) - 2\gamma \frac{de_0(\gamma)}{d\gamma} + \frac{1}{2}\gamma^2 \frac{d^2e_0(\gamma)}{d\gamma^2}}} \quad (51)$$

where v_s is sound velocity and v_N is stiffness which are defined as

$$v_s = \frac{L}{\pi\hbar} \frac{\partial^2 E}{\partial N^2}, \quad v_N = \sqrt{\frac{L^2}{mN} \frac{\partial^2 E}{\partial L^2}}. \quad (52)$$

In the above Eq. (51), the second expression of the Luttinger parameter is used for numerical calculation with the help of the Eq. (22).

Using the asymptotic expansion result of the ground state energy Eq. (24) for weak counting and Eq. (29) for the strong counting regimes, one find the asymptotic forms of the Luttinger parameter K for the two limits

$$K|_{\gamma \ll 1} = \pi \left(\gamma - \frac{1}{2\pi} \gamma^{3/2} \right)^{-1/2}, \quad (53)$$

$$K|_{\gamma \gg 1} = 1 + \frac{4}{\gamma} + \frac{4}{\gamma^2} - \frac{16\pi^2}{3\gamma^3}. \quad (54)$$

In the Fig. 6, we show that these asymptotic forms of the Luttinger parameters provide a very accurate expression throughout the whole parameter space. The correlation functions can be calculated by the conformal field theory [11, 30–32, 74].

Usually, the long distance or long time asymptotics of correlation functions of the 1D critical systems can be calculated by using the canonical field theory (CFT) [11]. From the CFT, the two-point correlation function for primary fields with the conformal dimensions Δ^\pm is given by [61]

$$G_O(y, \tau) = \sum \frac{Ae^{-2\pi i(N\Delta D)y/L}}{(v\tau + iy)^{2\Delta^+}(v\tau - iy)^{2\Delta^-}}, \quad (55)$$

where τ is the Euclidean time, v is the velocity of light, $G_O(x, t) = \langle G | \hat{O}^\dagger(x, t) \hat{O}(0, 0) | G \rangle$ is the correlator for the field operators $\hat{O}(0, 0)$ and $\hat{O}^\dagger(x, t)$. Eq. (55) involves the contributions of the excited states which are characterized by numbers ΔD , N^\pm and ΔN . Here N^- (or N^+) describes the elementary particle-hole excitations by moving atoms close to the left (or right) pseudo Fermi point outside the Fermi sea with adding N^- (or N^+) holes below the left (or right) Fermi point. ΔN is the change of particle number and it characterizes the elementary excitations by adding (or removing) particles over the ground state. N^\pm and ΔN are not enough to describe all elementary excitations. It is necessary to introduce the quantum number $2\Delta D$ to denote the particle number difference between the right- and left going particles. From the analysis of finite-size corrections of

the BAE, the total momentum and excited energy of the low-lying excitations in terms of these quantum numbers N^\pm , ΔN and D are given by

$$\Delta P = \frac{2\pi}{L} [\Delta N \Delta D + N^+ - N^-] + 2\Delta D k_F, \quad (56)$$

$$\Delta E = \frac{2\pi v}{L} \left[\frac{1}{4} (\Delta N/Z)^2 + (\Delta D Z)^2 + N^+ + N^- \right], \quad (57)$$

where $Z = 2\pi\rho(Q)$ is the dressed charge at the pseudo Fermi point for the ground state. From the conformal field theory, the excited energy and momentum are given by

$$\Delta E = \frac{2\pi v}{L} v(\Delta^+ + \Delta^-), \quad (58)$$

$$\Delta P = \frac{2\pi}{L} \sum_{\alpha} (\Delta^+ - \Delta^-) + 2\Delta D k_F, \quad (59)$$

By the comparison between the two results obtained from finite-size corrections (56), (57) and CFT (58), (59), the conformal dimensions are analytically obtained as a function of N^\pm , ΔN , ΔD and the dressed charge Z as well, namely,

$$2\Delta^\pm = 2N^\pm \pm \Delta N \Delta D + (\Delta D Z)^2 + \frac{1}{4} (Z^{-1} \Delta N)^2, \quad (60)$$

It turns out that only the low energy excitations determine the long distance or time asymptotic behavior of the correlation functions. For the operator $\hat{\psi}(x)$ being a prime operator of this $U(1)$ symmetric system, the correlation functions of the prime field have a universal power law decay in distance

$$\langle \hat{\psi}^\dagger(\tau, y) \hat{\psi}(0, 0) \rangle = \frac{\exp(2i\Delta D k_F y)}{(v\tau + iy)^{2\Delta^+} (v\tau - iy)^{2\Delta^-}}. \quad (61)$$

We find that Luttinger parameter $K = Z^2$ by the comparison to the result of Luttinger theory, $\langle \hat{\psi}^\dagger(y) \hat{\psi}(0) \rangle \sim 1/y^{1/2K}$. For example, at the strong coupling regime, the dressed charge $Z = 1 + 2/\gamma - 8\pi^2/3\gamma^3$ from the dressed charge equation [11]. Submitting it into $K = Z^2$, we get the same result as Eq. (54).

IV. YANG-YANG THERMODYNAMICS AND QUANTUM CRITICALITY

In 1969, C. N. Yang and C. P. Yang presented a grand canonical ensemble to describe finite temperature thermodynamics for the Lieb-Linger model [4]. The Yang-Yang method has led significant developments in quantum integrable systems [12, 13, 29]. This approach allows one to access full finite temperature physics of the models in terms of the thermodynamic Bethe ansatz (TBA)

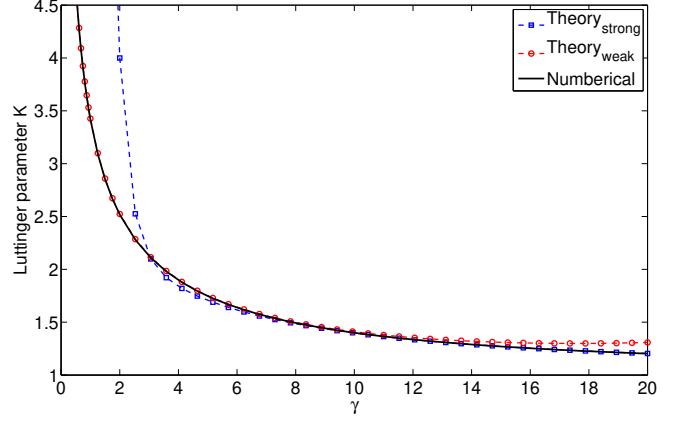


FIG. 6. (Color online) Luttinger parameter K vs interaction strength γ : the blue dashed line is the result Eq.(54) for the strong coupling limit. Whereas the red dashed line is the result Eq.(53) for weak coupling regime. The black solid line is the numerical result obtained from the Eq.(51). The analytical result of the Luttinger parameter is seen in a good agreement with the numerical result.

equations [12]. In the grand canonical ensemble, we usually convert the TBA equations in terms of the dimensionless chemical potential $\tilde{\mu} = \mu/c^2$ and the dimensionless temperature $\tilde{T} = T/c^2$ with the interaction strength c . It is also convenient to use the degenerate temperature as an energy unit, i.e. $T_d = \hbar^2 n^2/2m$ [21]. It is very insightful to discuss critical phenomena of the models in terms of the dimensionless units. We first discuss the Yang-Yang grand canonical ensemble below.

IV.1 The Yang-Yang grand canonical ensemble

For the ground state the set of quantum numbers (18) provides the lowest energy. However, at finite temperatures, any thermal equilibrium state involves many microscopic eigenstates. As discussed in previous section, these eigenstates are characterized by different quantum numbers $\{I_j\}$, see Eq. (16). In the thermodynamic limit, $I(k)$ is a monotonic function of pseudo momenta k [11]. We define $dI(k)/(Ldk) = \rho(k) + \rho_h(k)$, where ρ_h is the density of the holes. From the Eq. (16), we can get the integral BAE for arbitrary eigenstate as

$$\rho(k) + \rho_h(k) = \frac{1}{2\pi} + \int_{-\infty}^{\infty} a(k-k') \rho(k') dk'. \quad (62)$$

Here we should notice that integral interval can extend to the whole real axis, i.e. particles can occupy any real quasimomentum.

In order to understand the equilibrium states of the model, it is essential to introduce the entropy. In a small interval dk , the number of total vacancies is $L[\rho(k) + \rho_h(k)]dk$ with a number of $L\rho(k)dk$ particles

and a number of $L\rho_h(k)dk$ holes. These particles and holes give rise to microscopic states

$$dW = \frac{[L(\rho(k) + \rho_h(k))dk]!}{[L\rho(k)dk]![L\rho_h(k)dk]!}.$$

In the thermodynamic limit, $[L(\rho(k) + \rho_h(k))dk] \gg 1$ and $dk \rightarrow 0$, with the help of the Stirling's formula, the entropy in this small interval is given by

$$dS = \ln dW \approx L\{\rho \ln[1 + \eta] + \rho_h \ln[1 + \eta^{-1}]\}dk,$$

where $\eta(k) = \rho_h(k)/\rho(k)$. The total entropy is $S = \int dS$. It can be understood from this procedure that the entropy involves the disorder of mixing the particles and holes in the pseudo momentum space. For regions with zero $\rho(k)$ or zero $\rho_h(k)$, no disorder occurs, i.e. $dS = 0$. Therefore the entropy for the ground state is zero. It is worth noting that the above discussion is valid only in the equilibrium state.

The Gibbs free energy Ω is the thermodynamic potential of grand canonical ensemble for this model,

$$\Omega = E - TS - \mu N, \quad (63)$$

where μ is the chemical potential and the particle number is given by $N = L \int \rho(k)dk$. In thermal equilibrium, the true physical state is determined by the conditions of minimizing the Gibbs free energy. Making a virtual change $\delta\rho, \delta\rho_h$ in the thermal equivalent state, one take the variation of the free energy such that

$$\delta\Omega = \delta E - T\delta S - \mu\delta N = 0.$$

Here we should notice that the variations $\delta\rho$ and $\delta\rho_h$ are not independent in view of the integral BAE (62). This minimization condition leads to the TBA equations in term of the dressed energy [4]

$$\varepsilon(k) = k^2 - \mu + \int_{-\infty}^{\infty} a(k - k')\varepsilon_-(k')dk'. \quad (64)$$

Where the dressed energy is defined by $\varepsilon(k) = T \ln \eta(k)$. In the above equation, we also denoted $\varepsilon_-(k) = -T \ln[1 + e^{-\varepsilon(k)/T}]$. Using the TBA equation (64), we further obtained the grand thermodynamic potential $\Omega = \frac{TL}{2\pi} \int \varepsilon_-(k)dk$. It follows that the pressure is given by

$$p = -\left(\frac{\partial\Omega}{\partial L}\right)_{\mu,c,T} = -\frac{T}{2\pi} \int \varepsilon_-(k)dk. \quad (65)$$

This serves as the equation of state (65) from which we can calculate the thermodynamics of this model at finite temperatures. We can obtain the zero temperature and finite temperature phase diagrams of the Lieb-Liniger model. In the zero temperature limit, the TBA Eq. (64) reduces to the dressed energy equation Eq. (38) in the limit $T \rightarrow 0$. From the standard thermodynamic relations, one can calculate the particle density

$n = \partial_\mu p|_{c,T}$, entropy density $s = \partial_T p|_{\mu,c}$, compressibility $\kappa^* = \partial_\mu^2 p|_{c,T}$, specific heat $c_v = T\partial_T^2 p|_{\mu,c}$ in a straightforward way.

In view of the grand canonical ensemble, there exists a quantum phase transition at the chemical potential $\mu_c = 0$ at zero temperature. Universal thermodynamics is expected for the temperature under the quantum degenerate regime $T \lesssim T_d$, where $T_d = \hbar^2 n^2 / 2m$ [21]. At high temperatures (HT), i.e. $T \gg T_d$, the system behaves like a classical Boltzmann gas. For $\mu < \mu_c = 0$ and at the low temperatures, the density is very low and the gas becomes de-coherent. This phase is semi-classical (SC). Whereas for $\mu > \mu_c$ and the temperature $T < |\mu - \mu_c|$, it shows the Tomonaga-Luttinger liquid (TLL) phase. The quantum critical regime lies in between SC and TLL for the temperature $T \gg |\mu - \mu_c|$. We show such different regimes through the entropy and specific heat in Fig. 7.

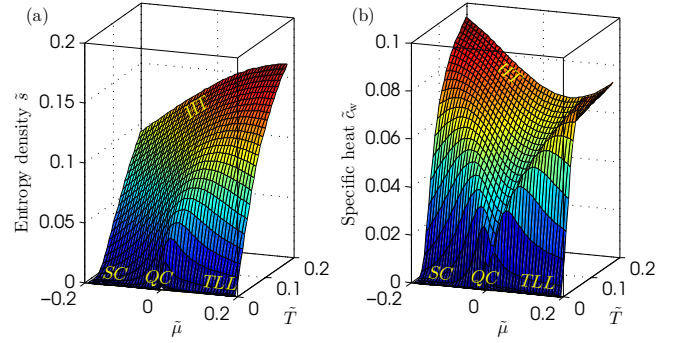


FIG. 7. (Color online) Quantum critical regimes for the Lieb-Liniger model. (a) and (b) show the dimensionless entropy and specific heat in the \tilde{T} - $\tilde{\mu}$ plane, respectively. For $\tilde{T} \gg 1$, it is the HT regime. The TLL with the dynamical exponent $z = 2$ and correlation length exponent $\nu = 1$ lies in the region $\tilde{T} \ll 1$ and $\mu > \mu_c$. For $\tilde{T} \gg |\mu - \mu_c|$, the QC regime with $z = 2$, $d = 1$ and $\nu = 1/2$ fans out near the quantum phase transition point $\tilde{\mu}_c = 0$. It is obvious that the entropy and the specific heat have singularity properties near the critical point $\mu_c = 0$.

IV.2 The Yang-Yang equation and quantum statistics

Dynamical interaction and thermal fluctuation drive Lieb-Liniger model from one phase into another. In particular, under the degenerate temperature T_d , the model has three distinct phases: semi-classical, quantum critical and the TLL critical phases. At high temperatures, there does not exhibit universal behaviour. For the temperature tends to infinity, the system reaches to the Boltzmann gas. Therefore the Yang-Yang equation (64) encodes different quantum statistics. For example, when the coupling strength $\gamma \rightarrow 0$, the system behaves as the

free bosons; for the strong coupling limit, it behaves like free fermions; at high temperatures, the system becomes the Boltzmann gas. In the following, we rigorously derive such quantum statistics in an analytical way.

When the coupling strength γ turn to zero, the integral kernel $a(k) \rightarrow \delta(x)$. The dressed energy in this limit can be expressed as

$$\lim_{c \rightarrow 0} \varepsilon(k) = T \ln [e^{(k^2 - \mu)/T} - 1] \quad (66)$$

from which we obtain the thermal potential per length $\lim_{c \rightarrow 0} \Omega/L = \int_0^\infty 2\sqrt{\epsilon}/[e^{(\epsilon - \mu)/T} - 1] d\epsilon$. Thus the distribution function satisfies the Bose-Einstein statistics

$$\lim_{c \rightarrow 0} g(\epsilon) = \frac{1}{e^{(\epsilon - \mu)/T} - 1}. \quad (67)$$

If $\gamma \rightarrow \infty$, the dressed energy reads

$$\lim_{c \rightarrow \infty} \varepsilon(k) = k^2 - \mu. \quad (68)$$

In this limit, the Bethe ansatz equation (62) naturally reduces to the form

$$\rho(k) = \frac{1}{2\pi(1 + \rho_h(k)/\rho(k))} \quad (69)$$

that indicates the Fermi-Dirac statistics. Consequently, the thermal potential per unit length is given by $\lim_{c \rightarrow \infty} \Omega/L = \int_0^\infty 2\sqrt{\epsilon}/[e^{(\epsilon - \mu)/T} + 1] d\epsilon$. This result gives rise to the Fermi-Dirac statistics

$$\lim_{c \rightarrow \infty} g(\epsilon) = \frac{1}{e^{(\epsilon - \mu)/T} + 1}. \quad (70)$$

We further remark that, eqs. (66-70) are valid for arbitrary temperature. If the system is under the quantum degeneracy, the quantum statistical interaction is important. Thus the particles are *indistinguishable*. At high temperatures the Yang-Yang equation (64) give rise to the Maxwell-Boltzmann statistic such that the particles are *distinguishable*. In the weak coupling limit and high temperature limits, it is very convenient to consider Virial expansions with the Yang-Yang equation (64), namely

$$e^{-\epsilon(k)/T} = \mathcal{Z} e^{-\frac{k^2}{T}} e^{\int_{-\infty}^{\infty} dq a(k-q) \ln \left(1 + \mathcal{Z} e^{-\frac{q^2}{T}} \right)}. \quad (71)$$

Here $\mathcal{Z} = e^{\mu/T}$ is fugacity. After some algebra, we find the pressure up to the second Virial coefficient is given by

$$p = p_0 + \frac{T^{\frac{3}{2}}}{\sqrt{2\pi}} \mathcal{Z}^2 p_2, \quad (72)$$

where $p_2 = -\frac{1}{2} + \int_{-\infty}^{\infty} dq' a(2q') e^{-\frac{2q'^2}{T}}$ reveals the two-body interaction effect. In the above equation, the $p_0 = -\frac{T}{2\pi} \int_{-\infty}^{\infty} dk \ln \left(1 - \mathcal{Z} e^{-\frac{k^2}{T}} \right)$ is the pressure of the free bosons. The result (72) gives the Maxwell-Boltzmann statistics in the limit of $T \rightarrow \infty$.

It is remarkable to discover the universal low temperature behavior of the Lieb-Liniger model with the Bose-Einstein statistic and Fermi-Dirac statistic. The Yang-Yang equation (64) provide full physics of the Lieb-Liniger model that goes beyond what can be found by Bose-Fermi mapping [16]. In fact, for strong coupling limit, i.e. $\gamma \gg 1$, the system can be viewed as an ideal gas with the fractional statistics [24]. When the coupling strength is very weak, the ground state behaves like a quasi BEC. The Bogoliubov approach is valid in the weak coupling limit $\tilde{T} \ll \sqrt{\gamma} \ll 1$ [21, 25]. The result (72) is also a good approximation for the weak coupling Lieb-Liniger gas.

IV.3 Luttinger liquid and quantum criticality

Equation of state

In low energy physics, $T \ll T_d$, low-lying excitations form a collective motion of bosons. The linear relativistic dispersion near the Fermi points results in the TLL behavior. At finite temperatures, the TLL can be sustained in a region of $T < |\mu - \mu_c|$ in the T - μ plane, see Fig. 7. In the TLL phase, one can take the Sommerfeld expansion with the TBA equation (64). By iterations, the pressure with the leading order temperature correction is given by

$$p = p_0 + \frac{\pi^2 T^2}{3} \frac{\rho_0(Q)}{\varepsilon'(Q)} = p_0 + \frac{\pi T^2}{6v_s}, \quad (73)$$

that gives the free energy per unit length as the field theory prediction

$$F(T)/L = \mu n - p \approx E_0 - \frac{\pi C (k_B T)^2}{6\hbar v_s} \quad (74)$$

with the central charge $C = 1$. Here we took $k_B = 1$. So that in TLL phase the specific heat is linear temperature-dependent

$$c_v = \frac{\pi T}{3v_s}. \quad (75)$$

This is an universal signature of the TLL.

However, for the temperature beyond the crossover temperature, i.e. $T > T^* \sim |\mu - \mu_c|$, the excitations give a non-relativistic dispersion, i.e. $\Delta E \sim p^2$. The crossover temperature T^* can be also determined by the breakdown of linear-temperature-dependent relation given by Eq. (75) [26]. The crossover is also evidenced by the correlation length, see recent work [35].

For strong coupling and low temperatures, i.e. $\gamma \gg 1$ and $\tilde{T} \ll 1$, the pressure is given by [26]

$$p = -\frac{T^{3/2}}{2\sqrt{\pi}} \text{Li}_{\frac{3}{2}}(-e^{A/T}) \left[1 + \frac{T^{3/2}}{2\sqrt{\pi} c^3} \text{Li}_{\frac{3}{2}}(-e^{A/T}) \right]. \quad (76)$$

where $A = \mu - \frac{2p}{c} + \frac{T^{5/2}}{2\sqrt{\pi}c^3} \text{Li}_{\frac{3}{2}}(-e^{A/T})$ and the polylogarithm function is given by $\text{Li}_n(x) = \sum_{k=1}^{\infty} \frac{x^k}{k^n}$. In the

above equation, the pressure p gives a close form of the equation of state. Using the standard thermodynamical relations, one can analytically calculate the particle density, compressibility and the specific heat

$$n = -\frac{1}{2\sqrt{\pi}} T^{\frac{1}{2}} f_{\frac{1}{2}} \left\{ 1 - \frac{1}{\sqrt{\pi}c} T^{\frac{1}{2}} f_{\frac{1}{2}} + \frac{T}{\pi c^2} f_{\frac{1}{2}}^2 + \frac{1}{\sqrt{\pi}c^3} T^{\frac{3}{2}} \left[-\frac{1}{\pi} f_{\frac{1}{2}}^3 + \frac{3}{2} f_{\frac{3}{2}} \right] \right\} \quad (77)$$

$$\kappa^* \approx -\frac{1}{2\sqrt{\pi}} T^{-\frac{1}{2}} f_{-\frac{1}{2}} + \frac{3}{2\pi c} f_{-\frac{1}{2}} f_{\frac{1}{2}} - \frac{2}{\pi^{3/2} c^2} T^{\frac{1}{2}} f_{-\frac{1}{2}} f_{\frac{1}{2}}^2 - \frac{1}{\pi c^3} T f_{-\frac{1}{2}} f_{\frac{3}{2}} + \frac{5}{\pi^2 c^3} T f_{-\frac{1}{2}} f_{\frac{1}{2}}^3 - \frac{3}{4\pi c^3} T f_{\frac{1}{2}}^2 \quad (78)$$

$$c_v = T \left(\frac{\partial s}{\partial T} \right)_{\mu, c} = -\frac{3}{8\sqrt{\pi}} T^{-\frac{1}{2}} f_{\frac{3}{2}} + \frac{3}{2\sqrt{\pi}} T^{-\frac{1}{2}} \frac{A}{T} f_{\frac{1}{2}} - \frac{1}{2\sqrt{\pi}} T^{-\frac{1}{2}} \left(\frac{A}{T} \right)^2 f_{-\frac{1}{2}} + O\left(\frac{1}{c}\right), \quad (79)$$

respectively. Here $f_n = \text{Li}_n(-e^{A/T})$.

Quantum criticality

At zero temperature the quantum phase transition from the vacuum phase into the TLL at the critical point $\mu_c = 0$ occurs in the Lieb-Liniger Bose gas. According to the renormalized group theory, universal scaling properties are expected in the critical regime at low temperatures, see Fig. 7. In 2011, Guan and Batchelor investigated quantum criticality of the Bose gas and found that the equation of state (76) reveals the universal scaling behaviour of quantum criticality in terms of the polylogarithm functions [26]. It is straightforward from the equation of the state to derive the universal scaling form of the density as

$$n(T, \mu) \approx n_0 + T^{d/z+1-1/\nu z} \mathcal{F}\left(\frac{\mu - \mu_c}{T^{1/\nu z}}\right), \quad (80)$$

where the background density $n_0 = 0$. The scaling function $\mathcal{F}(x) = -\frac{1}{2\sqrt{\pi}} \text{Li}_{\frac{1}{2}}(-e^x)$ read off the dynamic critical exponent $z = 2$, the correlation length exponent $\nu = 1/2$. It is particularly interesting that the finite temperature density profiles of the 1D trapped gas can map out the quantum criticality with these universal exponents for the Lieb-Liniger gas. The density curves at different temperatures intersect at the critical point, see Fig. 8 (a).

The universal scaling behaviour of compressibility κ^* is given by

$$\kappa^* = \kappa_0 + T^{d/z+1-2/\nu z} \mathcal{K}\left(\frac{\mu - \mu_c}{T^{1/\nu z}}\right), \quad (81)$$

where $\kappa_0 = 0$ and $\mathcal{Q}(x) = -\frac{1}{2\sqrt{\pi}} \text{Li}_{-\frac{1}{2}}(x)$. This scaling function again reads off the dynamic critical exponent $z = 2$, the correlation length exponent $\nu = 1/2$. The intersection at the critical point for different temperatures attributes the universal scaling form (81), see Fig. 8 (b).

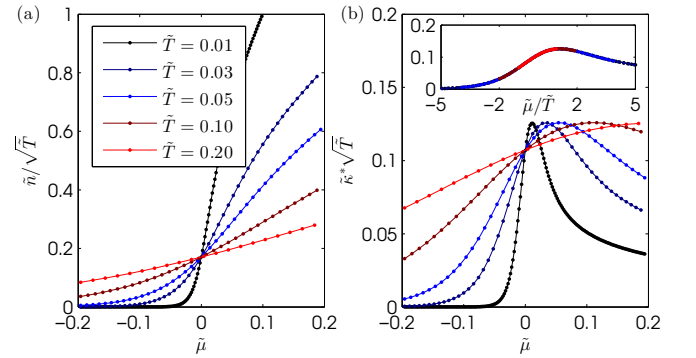


FIG. 8. (Color online) Universal scaling behaviours of the density and compressibility at quantum criticality. (a) The density shows the universal scaling behaviour given by (80). (b) The compressibility presents the universal scaling behaviour (81). The inset in (b) shows the collapse of temperature-rescaled compressibility $\kappa^* \sqrt{T}$ with respect to the argument $(\mu - \mu_c)/\tilde{T}$.

Near the critical point, the specific heat divided by the temperature $\tilde{c}_v \equiv c_v/T$ obeys the following scaling form

$$\tilde{c}_v = -T^{-\frac{1}{2}} \left[\frac{3}{8\sqrt{\pi}} \text{Li}_{\frac{3}{2}}(-e^{\frac{\mu}{T}}) - \frac{3}{2\sqrt{\pi}} \frac{\mu}{T} \text{Li}_{\frac{1}{2}}(-e^{\frac{\mu}{T}}) + \frac{1}{2\sqrt{\pi}} \left(\frac{\mu}{T} \right)^2 \text{Li}_{-\frac{1}{2}}(-e^{\frac{\mu}{T}}) \right] \quad (82)$$

The specific heat at different temperatures has two round peaks near the critical point $\mu_c = 0$. These peaks mark the crossover temperatures that distinguish the TLL and semi-classical gas phases from the quantum critical regime. This is a very robust signature for the existence of the crossover temperatures in the 1D Bose gas. This scaling law of the entropy and specific heat is shown in Fig. 9.

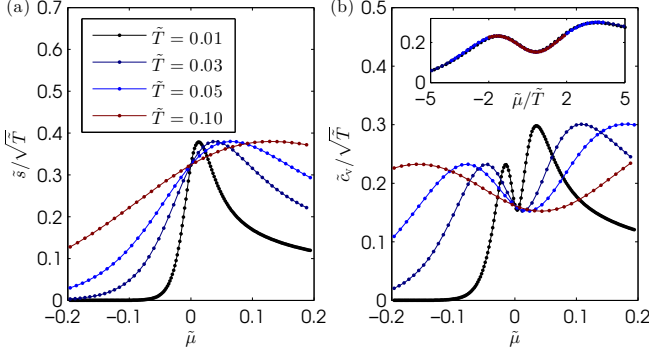


FIG. 9. (Color online) Quantum critical behaviour of the entropy and specific heat. (a) The entropy divided by temperature $\tilde{s} = s/T$ has a universal scaling behavior at the quantum criticality. (b) specific heat divided by temperature $\tilde{c}_v = c_v/T$ has a universal scaling behavior at the quantum criticality. The inset in (b) shows the collapse of $\tilde{c}_v/\sqrt{\tilde{T}}$ with respect to the argument $(\tilde{\mu} - \tilde{\mu}_c)/\tilde{T}$.

IV.4 The local pair correlations and Tan's Contact

In the study of the interacting Bose gas in one dimension, an important property is the local two-body correlation function g_2 . Physically speaking, this function describes the rates of inelastic collision between pairs of particles [76, 77]. This quantity reflects the probability that the two particles site at the same size. It is also know as Contact that strikingly captures the universality of ultracold atoms. This has been described by the Tan's relations [80]. Tan's Contact, which measures the two-body correlations at short distances in dilute systems, is a central quantity to ultra cold atoms. It builds up universal relations among thermodynamic quantities such as the large momentum tail, energy, and dynamic structure factor, through the renowned Tan's relations, see recent development in this research [27].

Knowing that the two-body correlation can lead to the classification of physically distinct regimes, for example, the Tonks-Girardeau regime with $g_2 \rightarrow 0$, the Gross-Pitaevskii regime with $g_2 = 1$ and the very weak coupling or fully decoherent regime with $g_2 = 2$. The two-body correlation function can be calculated for these different regimes by expression $g_2 = \langle \hat{\Psi}^\dagger(x) \hat{\Psi}^\dagger(x) \hat{\Psi}(x) \hat{\Psi}(x) \rangle$. Where $\hat{\Psi}$ is the field operator in second quantization. At $T = 0$, we have $dE_0/dc = Lg_2$, here E_0 is the ground state energy. For weak coupling limit, the local pair correlation $g_2/n^2 = 1 - \frac{2\sqrt{\gamma}}{\pi}$. For strong coupling limit, $g_2/n^2 = \frac{4\pi^2}{3\gamma^2} \left(1 - \frac{6}{\gamma}\right)$. In general, the local pair correlation can be used to study phase coherence behaviour at finite temperatures. Introducing the free energy per particle, i.e. $f(\gamma, T) = F/N$, the normalized two-particle

TABLE I. Experiments of Lieb-Liniger gas

quantum dynamics	⁸⁷ Rb [42, 52, 58, 59, 94]
thermalization	⁸⁷ Rb [42, 51, 58, 59]
solitons	⁸⁷ Rb [49, 60]
fermionization	³⁹ K [38, 53]
YY thermodynamics	⁸⁷ Rb [36, 37, 42, 43, 46–48]
strong coupling	⁸⁷ Rb [22, 23]
phase diagram	Cs [57]
3-body correlations	⁸⁷ Rb [39, 44], Cs [41]
excited state.	Cs [45]

local correlation is defined as

$$g_2 = \frac{\langle \hat{\Psi}^\dagger(x) \hat{\Psi}^\dagger(x) \hat{\Psi}(x) \hat{\Psi}(x) \rangle}{n^2} = \frac{2m}{\hbar^2 n^2} \left(\frac{\partial f(\gamma, T)}{\partial \gamma} \right) \Big|_{n, T}. \quad (83)$$

For strong coupling regime, the local pair correlation function is obtained from the equation of state [77–79]

$$g_2 = \frac{4\pi^2}{3\gamma^2} \left(1 - \frac{6}{\gamma} + \frac{T^2}{4\pi^2 T_d^2} \right). \quad (84)$$

On the other hand, in one dimension the fundamental thermodynamic relation in a harmonic trap is given by [27]

$$dp = n d\mu + s dT - \frac{\rho_s}{2} dw^2 - \mathcal{C} da_{1D} \quad (85)$$

where ρ_s and \mathcal{C} are the densities of superfluid and contact respectively. In this relation, $w = v_s - v_n$ is the difference between the velocity of the superfluid and normal components. Maxwell relations build the general connections between the Contact and other physical quantities such as

$$\begin{aligned} \left(\frac{\partial \mathcal{C}}{\partial \mu} \right)_{T, a_{1D}} &= - \left(\frac{\partial n}{\partial a_{1D}} \right)_{\mu, T}, \\ \left(\frac{\partial \mathcal{C}}{\partial T} \right)_{\mu, a_{1D}} &= - \left(\frac{\partial s}{\partial a_{1D}} \right)_{\mu, T}. \end{aligned}$$

Furthermore, one can obtain the Contact through the following relations

$$\mathcal{C} = -\frac{1}{c^2} \left(\frac{\partial p}{\partial c} \right)_{\mu, T} \approx \frac{1}{2\pi} T^2 f_{\frac{1}{2}} f_{\frac{3}{2}} \left(1 - \frac{1}{\sqrt{\pi c}} T^{\frac{1}{2}} f_{\frac{1}{2}} \right) \quad (86)$$

The Tan's Contact of the Lieb-Liniger gas does not has the usual scaling behaviour which was found for the interacting Fermi gas in [27]. This is mainly because the critical field $\mu_c = 0$ which doesn't depend on the scattering length a_{1D} , see Fig. 10.

V. EXPERIMENTAL DEVELOPMENT RELATED TO THE LIEB-LINIGER GAS

Over the past few decades, experimental achievements in trapping and cooling ultra cold atomic gases have revealed beautiful physics of the cold quantum world. In

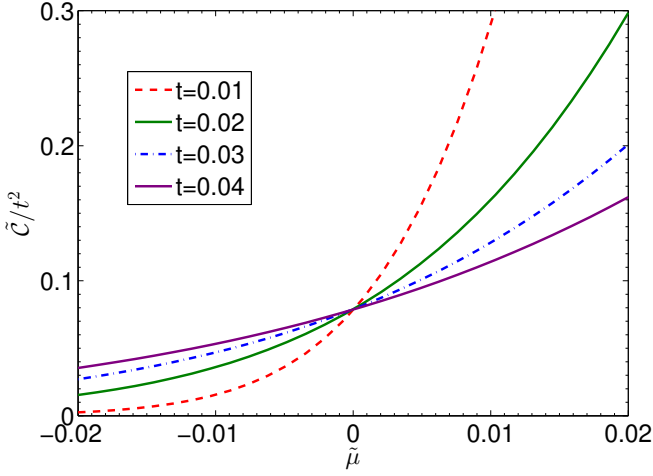


FIG. 10. (Color online) Contact divided by T^2 vs chemical potential. The critical scaling behaviour of the Contact for the Lieb-Liniger gas is different from the one for the 1D interacting Fermi gas [27].

particular, recent breakthrough experiments on trapped ultracold bosonic and fermionic atoms confined to one dimension have provided a precise understanding of significant quantum statistical and strong correlation effects in quantum many-body systems. The particles in the waveguides are tightly confined in two transverse directions and weakly confined in the axial direction. The transverse excitations are fully suppressed by the tight confinements. Thus the atoms in these waveguides can be effectively characterised by a quasi-1D system. Thus 1D effective interaction potentials can be controlled in the whole interacting regime by the underlying 3D scattering with tight confinements in the two transverse directions [28]. In such a way, these 1D many-body systems ultimately relate to the integrable models of interacting bosons and fermions. It is now possible to realize effectively one-dimensional quantum Bose gases in which the interaction strength between ultracold atoms is tunable, see recent reviews [29, 30]. These experiments have successfully demonstrated the anisotropic confinements of atoms to one dimension by optical waveguides, see a feature review article [34]. Particularly striking examples involve the measurements of momentum distribution profiles [22, 36], the ground state of the Tonks-Girardeau gas [23], quantum correlations [37–42], Yang-Yang thermodynamics [43, 44], the super Tonks-Girardeau gas [45], quantum phonon fluctuations [46–48], elementary excitations and dark solitons [49, 50], thermalization and quantum dynamics [51–53]. More experimental developments of the Lieb-Liniger model are listed in Table I [81].

The early experimental studies of the Lieb-Liniger gas with cold atoms were made in the lab by Immanuel Bloch's group [22] and David S Weiss's group [23]. In

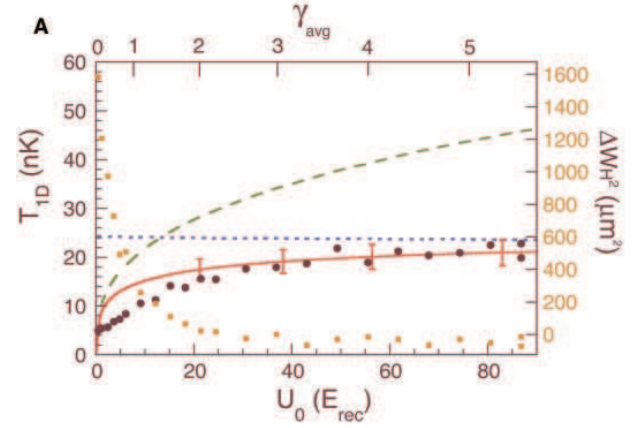


FIG. 11. (Color online) The 1D ground state energy T_{1D} vs transverse confinement depth of the lattice. For the confinement potential $U_0 > 0$ (or say the effective interaction $\gamma \gg 1$) the energy T_{1D} well presents the ground state energy of the Lieb-Liniger gas in strong coupling regime within the local density approximation. Figure extracted from [23].

particular, the observation of the ground state energy of the Tonks-Girardeau gas provides deep insights into understanding fermionization effect induced by a strong repulsive interaction, see Fig. 11. Loading the ^{87}Rb ultracold atoms into a 2D array of 1D tubes, where the atoms were kept in the lowest energy state in the two transverse directions. Thus the systems were realized in quasi-1D systems within axial harmonic traps. The essential feature of the Tonks-Girardeau gas was observed through the ground state energy T_{1D} of such waveguided ensembles.

The experimental measurement of the metastable highly excited state - the super Tonks-Girardeau gas was achieved by Haller [45] in 2009. They made a new experimental breakthrough with a stable highly excited gas-like phase in the strongly attractive regime of bosonic Cesium atoms across a confinement-induced resonance, see Fig. 12. This particular state was first predicted theoretically by Astrakharchik et al. [62] using the Monte Carlo method and by ANU group from the integrable interacting Bose gas with attractive interactions [63]. This model has improved our understanding of quantum statistics and dynamical interaction effect in many-body physics. It turns out that an highly excited state of gas-like gas could be stable as switching the interaction from strongly repulsive into strongly attractive interactions due to the existence of Fermi-like pressure [64–66]. This phenomenon has triggered much attention in theory [68].

In fact, many experiments have successfully demonstrated the confinements of atoms to one dimension by optical waveguides. Another particularly interesting example involves the measurement of photoassociation rates in one-dimensional Bose gases of ^{87}Rb atoms to determine the local pair correlation function $g^{(2)}(0)$ over a

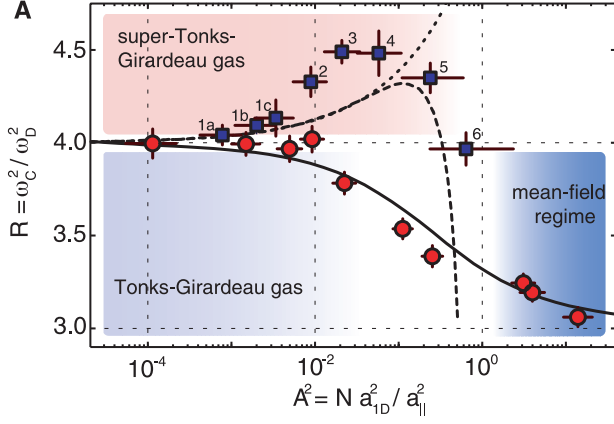


FIG. 12. (Color online) The ratio of compress mode over the trapping frequency $R = \omega_c^2/\omega_D^2$ vs the interaction parameter A^2 . The squares show the experimental measurements in strong attractive regime. The circles show the experimental data ranging from weak coupling to strong TG regimes. The black solid line stands for the exact result from the Lieb-Linger gas with a repulsion. The dashed lines present the theoretical data from the result [62]. Further study of the Tonks-Girardeau gas can be found in [64]. Figure extracted from [45].

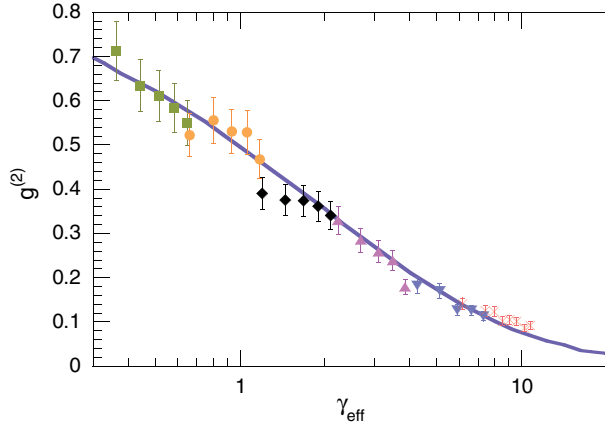


FIG. 13. (Color online) The local pair correlation function vs the effective coupling constant. The solid line is obtained from the exactly solved model of Lieb-Linger gas at zero temperature. The symbols show the experimental data. Figure extracted from [37].

range of interaction strengths, see Fig. 13. This experiment provides a direct observation of the fermionization of bosons with increasing interaction strength. It sheds light on the phase coherence behavior [21, 66, 69, 70]. At zero temperature the local pair correlation is $g^{(2)}(0) \sim 1$ for the weakly interacting Bose gas and $g^{(2)}(0) \rightarrow 0$ as the system enters into the Tonks-Girardeau regime.

As having been discussed in previous sections, the finite temperature problem of the Lieb-Liniger Bose gas was solved by Yang and Yang in 1969 [4]. It turns out

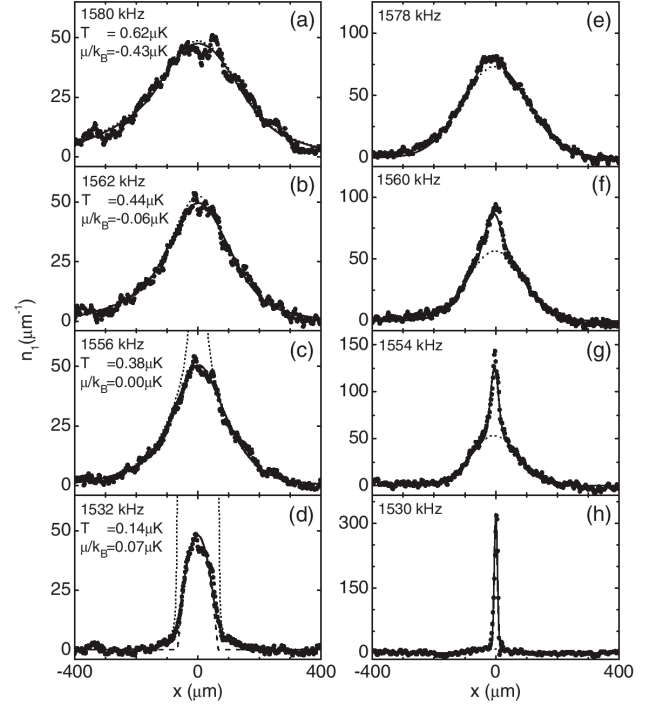


FIG. 14. The in situ axial density profiles for the weakly interaction Bose gas of ^{87}Rb atoms at different temperatures. The solid lines show the result obtained from the Yang-Yang equations. The values of the chemical potentials are indicated by the harmonically trapping potentials. The experimental data show a good agreement with the theoretical prediction from the Yang-Yang equation. Figure extracted from [37].

that the Yang-Yang thermodynamic equation is an elegant way to analytically access the thermodynamics, quantum fluctuations and quantum criticality. The Yang-Yang thermodynamics have been confirmed in the recent experiments through various thermodynamical properties [43, 44] and quantum fluctuations [46–48]. A typical example is the measurements of the Yang-Yang thermodynamics on the atom chip, see Fig. 14.

Moreover, recent experimental simulations with ultracold atoms provide promising opportunities to test quantum dynamics of many-body systems. In particular, nonequilibrium evolution of a isolated system involves transport and quench dynamics beyond the usual thermal Gibbs mechanism where the ground state and low lying excitation play an essential role. The experimental study [51, 52] of thermalization of 1D ensemble of cold atoms has led to a significant developments in this field [71, 72]. In these experiments, it was demonstrated that quench the dynamics into the isolated systems can lead to non-thermal distributions if conserved laws exist. So far a generalized Gibbs ensemble is believed to present the non-thermal distributions in the isolated systems with conserved laws. The many-body density matrix is writ-

ten

$$\hat{\rho} = \frac{1}{Z} \exp \left(- \sum_m \lambda_m \hat{\mathcal{I}}_m \right) \quad (87)$$

in terms of conserved quantities $\hat{\mathcal{I}}_m$. Here $Z = \text{Tr} \exp \left(- \sum_m \lambda_m \hat{\mathcal{I}}_m \right)$ is the partition function. The Lagrange multipliers λ_m acting for maximization of the entropy are determined by the associated conserved laws. The Fig. 15 shows the quantum Newton's cradle that provides an insightful signature of such a generalized Gibbs ensemble. It shows that the 1D systems with many-conserved laws do not approach to thermal equilibrium.

Recently, Langen et al [94] showed that a degenerate 1D Bose gas relaxes to a state that can be described by such a generalized Gibbs ensemble. By splitting a 1D Bose gas into two halves, they prepared a non-equilibrium system of ^{87}Rb atoms trapped in an atomic chip. They measured the local relative phase profile $\varphi(z)$ between the two halves. It was shown that most of the experimentally reachable initial states evolve in time into the steady states which can be determined within a reasonable precision by far less than N Lagrange multipliers. It was particularly interesting to see that the experimental data of the reduced χ^2 values can be well fitted with about 10 modes although there exists a much larger number of conserved quantities in the system. This research opens to further study of the generalized Gibbs ensemble for the quantum systems out of equilibrium.

VI. OUTLOOK

We have introduced a fundamental understanding of many-body phenomena in the Lieb-Liniger model. The exact results for various physical properties of the Lieb-Liniger model at $T=0$ and at finite temperature were obtained by using the Bethe ansatz equations. In particular, we have presented a precise understanding of the excitation modes, Luttinger liquid, quantum statistics, quantum criticality, correlations and dynamics in the context of Bethe ansatz. In fact, there have been great developments in the study of the Lieb-Liniger model in literature [11, 15, 30] via various methods such as field theory methods [66, 73], Luttinger liquid theory and bosonization etc [74, 75]. It was shown that the repulsive Lieb-Liniger Bose gas can be obtained as the nonrelativistic limit of the sinh-Gordon model [82, 83]. Moreover, the study of the non-thermal distributions for the isolated systems with many conserved laws has been attracted much attention. In this scenario, the generalized Gibbs ensemble [72, 84–87] has been used to study the thermalization of the isolated systems. More recently there have been a growing interests on quench dynamics in terms of the generalized Gibbs Ensemble, see [88–93], etc. This research has been becoming a new frontier in

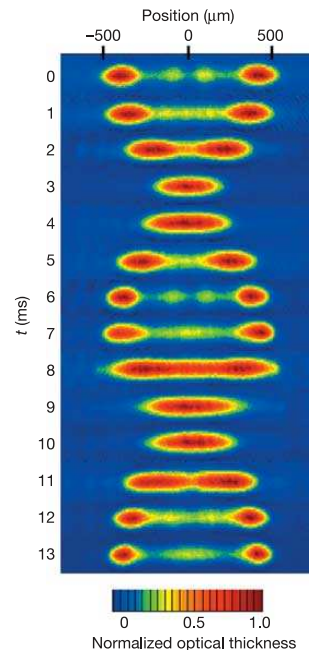


FIG. 15. (Color online) The time series of absorption images of the first oscillation cycle for initial average peak coupling strength $r_0 = 1$. The two groups of the cold atoms were confined into one dimension and initially separated by grating pulses. They evolved from time to time and collided twice in the centre of the harmonic 1D trap in each full cycle. The oscillations in 1D Bose gas last for a long time, even without approaching equilibrium. Figure extracted from [51].

cold atoms and condensed matter physics. It turns out that the integrable systems of this kind thus provide a promising platform to advance the basic understanding of new quantum effects in many-body physics, such as few-body problems, universal thermodynamics, universal contact, quench dynamics and correlation functions. These studies will further place mathematical theories of exactly solvable models into the lab for a wide range of physical phenomena.

Acknowledgment. The author XWG thanks Murray T Batchelor, You-Jin Deng, Hui Zhai, Zhen-Sheng Yuan, Fei Zhou and Qi Zhou for helpful discussions. This work has been supported by the National Basic Research Program of China under Grant No. 2012CB922101 and NNSFC under grant numbers 11374331 and 11304357. He acknowledges the Department of Physics, Chinese University of Hong Kong for their kind hospitality.

* e-mail: xwe105@wipm.ac.cn

[1] This brief introduction to the Bethe ansatz solvable model is based on some informal lectures delivered by the author XWG at the University of Science and Tech-

- nology of China, and Institute for advanced Study at Tsinghua University.
- [2] Bethe H 1931 *Z. Physik* **71** 205
 - [3] Lieb E H and Liniger W 1963 *Phys. Rev.* **130** 1605
 - [4] Yang C N and Yang C P 1969 *J. Math. Phys.* **10** 1115
 - [5] Yang C N 1967 *Phys. Rev. Lett.* **19** 1312
 - [6] Gaudin M 1967 *Phys. Lett. A* **24** 55
 - [7] Baxter R J 1972 *Ann. Phys. (N.Y.)* **70** 193; 1972 *Ann. Phys. (N.Y.)* **70** 323
 - [8] Baxter R J 1982 *Exactly Solved Models in Statistical Mechanics* (London: Academic Press)
 - [9] Yang C N 1983 *Selected papers 1945-1980* W. H. Freeman and Company
 - [10] Yang C N 2013 *Selected papers II* World Scientific
 - [11] Korepin V E, Izergin A G Izergin and Bogoliubov N M 1993 *Quantum Inverse Scattering Method and Correlation Functions* (Cambridge: Cambridge University Press)
 - [12] Takahashi M 1999 *Thermodynamics of One-Dimensional Solvable Models* (Cambridge: Cambridge University Press)
 - [13] Essler F H L, Frahm H, Ghmann F, Klumper A and Korepin V E 2005 *The One-Dimensional Hubbard Model* (Cambridge: Cambridge University Press)
 - [14] Sutherland B 2004 *Beautiful Models* (Singapore: World Scientific)
 - [15] Gaudin M 2014 *The Bethe Wavefunction* (Cambridge: Cambridge University Press)
 - [16] Girardeau M, Nguyen H and Olshanii M 2004 *Opt. Commun.* **243** 3
 - [17] Gaudin M 1971 *Phys. Rev. A* **4** 386
 - [18] Iida T and Wadati M 2005 *J. Phys. Soc. Jpn.* **74** 1724-1736
 - [19] Batchelor M T, Guan X W and McGuire J B 2004 *J. Phys. A* **37** L497
 - [20] Bortz M private communications
 - [21] Gangardt D M and Shlyapnikov G V 2003 *Phys. Rev. Lett.* **90** 010401; Kheruntsyan K V, Gangardt D M, Drummond P D and Shlyapnikov G V 2003 *ibid* **91** 040403
 - [22] Paredes P 2004 *Nature (London)* **429** 277
 - [23] Kinoshita T, Wenger T and Weiss D S 2004 *Science* **305** 1125
 - [24] Batchelor M T and Guan X W 2007 *Laser Phys. Lett.* **4** 77
 - [25] Panfil M and Caux J S 2014 *Phys. Rev. A* **89** 033605
 - [26] Guan X W and Batchelor M T 2011 *J. Phys. A: Math. Theor.* **44** 102001
 - [27] Chen Y Y, Jiang Y Z, Guan X W and Zhou Q 2014 *Nature Commun.* **5** 51040
 - [28] Olshanii M 1998 *Phys. Rev. Lett.* **81** 938; Dunjko V, Lorent V and Olshanii M 2001 *Phys. Rev. Lett.* **86** 5413
 - [29] Guan X W, Batchelor M T and Lee C 2013 *Rev. Mod. Phys.* **85** 1633
 - [30] Cazalilla M A, Citro R, Giamarchi T, Orignac E and Rigol M 2011 *Rev. Mod. Phys.* **83** 1405
 - [31] Caux J S and Calabrese P 2006 *Phys. Rev. A* **74** 031605(R)
 - [32] Panfil M and Caux J S 2014 *Phys. Rev. A* **89** 033605
 - [33] Guan L M private communications
 - [34] Batchelor M T 2014 *Int. J. Mod. Phys. B* **28** 1430010
 - [35] Klumper A and Patu O I 2014 *Phys. Rev. A* **90** 053626
 - [36] Jacqmin T, Fang B, Berrada T, Rosclde T and Bouchoule I 2012 *Phys. Rev. A* **86** 043626
 - [37] Kinoshita T, Wenger T and Weiss D S 2005 *Phys. Rev. Lett.* **95** 190406
 - [38] Guarrera V, Muth D, Labouvie R, Vogler A, Barontini G, Fleischhauer M and Ott H 2012 *Phys. Rev. A* **86** 021601(R)
 - [39] Armijo J, Jacqmin T, Kheruntsyan and Bouchoule 2010 *Phys. Rev. Lett.* **105** 230402
 - [40] Tolra B L, O'Hara K M, Huckans J H, Phillips W D, Rolston S L and Porto J V 2004 *Phys. Rev. Lett.* **92** 190401
 - [41] Haller E, Rabie M, Mark M J, Danzl J G, Hart R, Lauber K, Pupillo G and Ngerl H C 2011 *Phys. Rev. Lett.* **107** 230404
 - [42] Kuhnert M, Geiger R, Langen T, Gring M, Rauer B, Kitagawa T, Demler E, Smith D A and Schmiedmayer J 2013 *Phys. Rev. Lett.* **110** 090405
 - [43] van Amerongen A H, van Es J J P, Wicke P, Kheruntsyan K V and van Druten N J 2008 *Phys. Rev. Lett.* **100** 090402
 - [44] Vogler A, Labouvie R, Stubenrauch F, Barontini G, Guarrera V and Ott H 2013 *Phys. Rev. A* **88** 031603(R)
 - [45] Haller E, Gustavss M, Mark M J, Danzl J G, Hart R, Pupillo G and Ngerl H C 2009 *Science* **325** 1224
 - [46] Jacqmin T, Armijo J, Berrada T, Kheruntsyan K V and Bouchoule I 2011 *Phys. Rev. Lett.* **106** 230405
 - [47] Esteve J, Trebbia J B, Schumm T, Aspect A, Westbrook C I and Bouchoule I 2006 *Phys. Rev. Lett.* **96** 130403
 - [48] Armijo J 2012 *Phys. Rev. Lett.* **108** 225306
 - [49] Karpiuk T, Deuar P, Bienias P, Witkowska E, Pawlowski K, Gajda M, Rzazewski K and Brewczyk M 2012 *Phys. Rev. Lett.* **109** 205302
 - [50] Fabbri N, Panfil M, Clment D, Fallani L, Inguscio M, Fort C and Caux J S 2014 arXiv:1406.2176v2 [cond-mat.quant-gas].
 - [51] Kinoshita T, Wenger T and Weiss D S 2006 *Nature* **440** 900
 - [52] Hofferberth S, Lesanovsky I, Fischer B, Schumm T and Schmiedmayer J 2007 *Nature* **449** 324
 - [53] Ronzheimer J P 2013 *Phys. Rev. Lett.* **110** 205301
 - [54] Kormos M, Mussardo G and Trombettoni A 2010 *Phys. Rev. A* **81** 043606
 - [55] Kormos M, Mussardo G and Pozsgay B 2010 *JSAT* P05014
 - [56] Kormos M, Mussardo G and Trombettoni A 2009 *Phys. Rev. Lett.* **103** 210404
 - [57] Haller E, Hart R, Mark M J, Danzl J G, Reichslner L, Gustavsson M, Dalmonte M, Pupillo G and Ngerl H C 2010 *Nature* **466** 597
 - [58] Langen T, Geiger R, Kuhnert M, Rauer B and Schmiedmayer J 2013 *Nature Phys.* **9** 640
 - [59] Stimming H P, Mauser N J, Schmiedmayer J and Mazets I E 2010 *Phys. Rev. Lett.* **105** 015301
 - [60] Witkowska E, Deuar P, Gajda M and Rzaewski K 2011 *Phys. Rev. Lett.* **106** 135301
 - [61] Belavin A A, Polyakov A M and Zamolodchikov A B 1984 *Nucl. Phys. B* **241** 333
 - [62] Astrakharchik G E, Boronat J, Casulleras and Giorgini S 2005 *Phys. Rev. Lett.* **95** 190407
 - [63] Batchelor M T, Bortz M, Guan X W and Oelkers N 2005 *J. Stat. Mech. : Theory Exp.* L10001
 - [64] Chen S, Guan L, Yin X, Hao Y and Guan X W 2010 *Phys. Rev. A* **81** 031609(R)
 - [65] Panfil M, Nardis J D and Caux J S 2013 *Phys. Rev. Lett.* **110** 125302

- [66] Kormos M, Mussardo G and Trombettoni A 2011 *Phys. Rev. A* **83** 013617
- [67] Girardeau M D and Astrakharchik G E 2009 *Phys. Rev. A* **81** 061601(R)
- [68] Guan X W 2014 *Int. J. Mod. Phys. B* **28** 1430015
- [69] Ristivojevic Z 2014 *Phys. Rev. Lett.* **113** 015301
- [70] Guan X W, Batchelor M T and Takahashi M 2007 *Phys. Rev. A* **76** 043617
- [71] Rigol M, Dunjko V, Yurovsky V and Olshanii M 2007 *Phys. Rev. Lett.* **98** 050405
- [72] Rigol M, Dunjko V and Olshanii M 2008 *Nature* **452** 854
- [73] Kormos M, Mussardo G and Trombettoni A 2009 *Phys. Rev. Lett.* **103** 210404; Kormos M, Chou Y Z and Imambekov A 2011 *Phys. Rev. Lett.* **107** 230405
- [74] Giamarchi T 2004 *Quantum Physics in One Dimension* (Cambridge: Cambridge University Press)
- [75] Cheianov V V, Smith H and Zvonarev M B 2006 *J. Stat. Mech. : Theory Exp.* P08015
- [76] Gangardt D M and Shlyapnikov G V 2003 *Phys. Rev. Lett.* **90** 010401
- [77] Kheruntsyan K V, Gangardt D M, Drummond P D and Shlyapnikov G V 2003 *Phys. Rev. Lett.* **91** 040403; 2005 *Phys. Rev. A* **71** 053615
- [78] Cazalilla M A 2003 *Phys. Rev. A* **67** 053606
- [79] Guan X W, Batchelor M T and Takahashi M 2007 *Phys. Rev. A* **76** 043617
- [80] Tan S 2008 *Ann. Phys.* **323** 2952; *Ann. Phys.* **323** 2971; *Ann. Phys.* **323** 2987
- [81] The experiments are chosen for the most relative to the Lieb-Liniger model, and by no means exhaustive.
- [82] Kormos M, Mussardo G and Trombettoni A 2010 *Phys. Rev. A* **81** 043606
- [83] Kormos M, Mussardo G and Pozsgay B 2010 *J. Stat. Mech. : Theory Exp.* P05014
- [84] Caux J S and Essler F H L 2013 *Phys. Rev. Lett.* **110** 257203
- [85] Nardis J, Wouters B, Brockmann M and Caux J S 2014 *Phys. Rev. A* **89** 033601
- [86] Goldstein G and Andrei N 2014 arXiv:1405.6365v1 [cond-mat.quant-gas]
- [87] Goldstein G and Andrei N 2013 arXiv:1309.3471v1 [cond-mat.quant-gas]
- [88] Lye D and Andrei N 2012 *Phys. Rev. Lett.* **109** 115304
- [89] Pozsgay B 2014 arXiv:1406.4613v2 [cond-mat.stat-mech]
- [90] Wouters B, Nardis J D, Brockmann M, Fioretto D, Rigol M and Caux J S 2014 *Phys. Rev. Lett.* **113** 117202
- [91] Brockmann M, Wouters B, Fioretto D, Nardis J D, Vlijm R and C J S 2014 *J. Stat. Mech.* P12009
- [92] Pozsgay B, Mestyn M, Werner M A, Kormos M, Zarnd G and Takcs G 2014 *Phys. Rev. Lett.* **113** 117203
- [93] Goldstein G and Andrei N 2014 arXiv:1405.4224v2 [cond-mat.quant-gas]
- [94] Langen T, Erne S, Geiger R, Rauer B, Schweigler T, Kuhnert M, Rohringer W, Mazets I E, Gasenzer T and Schmiedmayer J 2014 arXiv:1411.7185v1 [cond-mat.quant-gas]